A Review of SMA-based Actuators For Bidirectional Torsional Motion: Application To Origami Robots

Kejun Hu *, **Kanty Rabenorosoa and Morvan Ouisse**

Université Bourgogne Franche-Comté, FEMTO-ST Institute, CNRS/UFC/ENSMM/UTBM, Besançon 25000, France

Correspondence*:
Corresponding Author
kejun.hu@femto-st.fr

ABSTRACT

Shape memory alloys (SMAs) are a group of metallic alloys capable of sustaining large inelastic strains that can be recovered when subjected to a specific process between two distinct phases. Regarding their unique and outstanding properties, SMAs have drawn considerable attention in various domains and recently became appropriate candidates for origami robots, that require bi-directional torsional motion actuation with limited operational space. However, longitudinal motion-driven actuators are frequently investigated and commonly mentioned, but studies in SMA-based torsional motion actuation is still very limited in the literature. This work provides a review of different research efforts related to SMA-based actuators for bi-directional torsional motion (BTM), thus providing a survey and classification of current approaches and design tools that can be applied to origami robots in order to achieve shape-changing. For this purpose, analytical tools for description of actuator behaviour are presented, followed by characterization and performance prediction. Afterward, the actuators' design methods, sensing, and controlling strategies are discussed. Finally, open challenges are discussed.

Keywords: shape memory alloy, bi-directional torsional motion, origami robot, shape-changing, modelling

1 INTRODUCTION

Shape memory alloys (SMAs)[1] are a group of metallic alloys capable of sustaining large inelastic strains that can be recovered when subjected to a specific process between two distinct phases, which is temperature or magnetic field dependent. Two key behaviours of SMAs result from this transformation: shape memory effect (SME) and pseudoelasticity (PE) (Shaw et al., 2008). The former refers to the material's ability to recover large, seemingly permanent strains via thermal stimulus from a deformed shape in martensite to a 'memorized' one. The latter is associated with SMAs being able to undergo large, hysteretic stress-strain excursions without any permanent deformations at a sufficiently high temperature(Lester et al., 2015). Because of its (1) high energy density, (2) reasonable operational strain (Wei et al., 1998) rely to SME,

[1] Nitinol was first discovered by Buehler and colleagues in 1963 (Buehler et al., 1963), it is known as a conventional SMA.

(3) bio-compatibility, (4) long life [2] (Ikuta, 1990), the SMAs provide a good potential of development of advanced and inexpensive actuators (see table (1)), which could significantly reduce the mechanical complexity and size of structures. Over the last years, the demand for SMAs for engineering and technical applications has been increasing in numerous fields, such as in medical applications (Yoneyama and Miyazaki, 2008), structures and composites (Lester et al., 2015), automotives (Jani et al., 2014), aerospace (Hartl and Lagoudas, 2007; Benafan et al., 2019), and even robotics (Rodrigue et al., 2017).

Origami is a powerful method to introduce many unique and desirable structural properties such as auxetics,

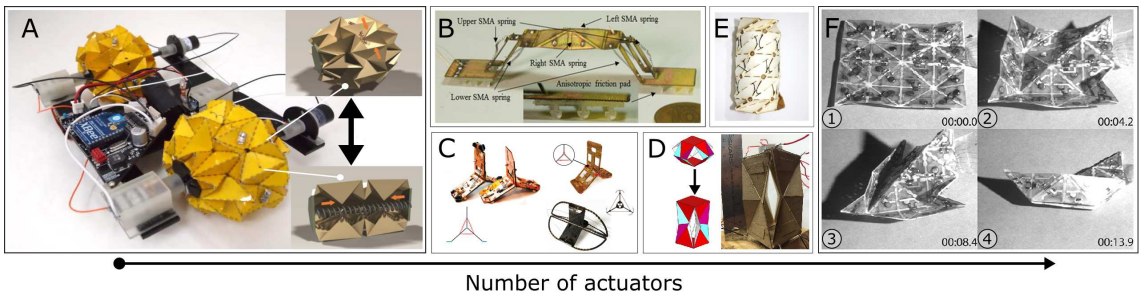

Figure 1. Diversity of SMA-Based origami robots. Origami robots arranged by the number of actuators: **(A)** a deformable wheel robot (Lee et al., 2013). **(B)** an inchworm-inspired crawling robot (Koh and Cho, 2013). **(C)** different versions of a bi-modal locomotion origami robot of Paik's group (Zhakypov et al., 2015; Zhakypov et al., 2017; Zhakypov and Paik, 2018). **(D)** a self-deployable lifting structure (Wood et al., 2016). **(E)** a 'shape switching' module with controllable stiffness (Kim et al., 2015a). **(F)** a '2D→3D' shape-morphing system (Hawkes et al., 2010).

tunable stiffness, multistability (Li et al., 2019; Kshad and Naguib, 2021). Robots inspired by folding mechanical structures known as 'Origami robots' gained much attention recently. As for the robotics field, the introduction of origami engineering enables 'semi-rigid' properties. In other words, they exhibit the properties of both rigid and soft robots. For example, origami robots can be precise and support high loads like rigid robots, and at the same time, they can be as dexterous and flexible as soft robots (Rus and Tolley, 2018). Moreover, the introduction of smart-material-based micro-actuators such as electro-active polymers (EAP) (Benouhiba et al., 2018) and SMA provides infinite possibilities to origami structures for self-deploying (Tolley et al., 2014; Wang et al., 2016) and dynamic shape-changing (Kim et al., 2016; Firouzeh and Paik, 2015). As shown in figure 1, coupling with SMA makes origami robots achieve various tasks such as large ratio volume changing (1A), multi-type local motion (1B and 1C), high load-lifting (1D and 1E) and complex shape-morphing (1E). However, longitudinal motion-driven actuators (for example, tensile or bending behaviour-based actuation) are frequently investigated and commonly mentioned, but studies in SMA-based torsional motion actuation is still very limited in the literature. Yuan et al. (2017b) presented a review on SMA-based rotary actuators. In this review, a classification based on actuators architecture and a variety of supplementary mechanisms had been carried out. Stroud and Hartl (2020) proposed a review of SMA-based torsional actuators focusing on applications in automotive and aeronautic domains, which usually require centimeter-size actuators. As indicated by Peraza Hernandez et al. (2014), the choice of actuators for self-folding structures, should be done according to criteria such as energy-density, simple geometry, and especially the actuators' compactness since systems at reference configurations are often essential. Table 1 shows a summary of principle performance of active material-based actuators. Base on the comparison, SMAs can offer a trade-off between advantages such as significant strain, stress, high work

[2] up to 10^6 action cycles under a strain of 1%

Table 1. Comparison of active materials' performance, inspired from (Bhandari et al., 2012; Mohd Jani et al., 2014; Wang et al., 2018)

Actuator type	Stress (MPa)	Strain (%)	Efficiency (%)	Bandwidth (Hz)	Work density (J/cm3)
NiTi SMA	200	10	3	3	10
Piezoceramic	35	0.2	50	5000	0.035
Single crystal piezoelectric	300	1.7	90	5800	2.55
Human Muscle	0.007–0.8	1–100	35	2–173	0.035
Hydraulic	20	50	80	4	5
Pneumatic	0.7	50	90	20	0.175
Ionic polymer-metal composites	0.3	40	30	0.1-100	0.0024
Dielectric electro-active polymer	2	100-380	60-90	1-10k	3.4

density, and inconvenience such as relatively low energy efficiency, low bandwidth. These properties make SMAs suitable candidates for origami robots' actuation. In the present study, thermally activated SMAs for bidirectional torsional motion (**BTM**) of meso-scale robotics are considered. This type of actuator is capable of providing torsional torque and rotation angle in two opposite directions for cyclic actuation using SME.

This paper aims at going over the different research efforts related to SMA-based actuators for BTM, thus providing a survey and classification of current approaches and design tools that might be applied to them. Specifically, the remainder of this paper is organized as follows: Section 2 presents a brief summary of SMA materials and describes how they might be used for actuation. Section 3 presents the classification of SMA element and a review of actuators' architecture for BTM. Section 4 provides a discussion based on the review, in terms of modeling, actuators' characterization, performance prediction and designing, activation strategies and sensing & controlling methods.

2 BRIEF SUMMARY OF SMA

2.1 SMA's thermal mechanical behaviour

Shape memory alloys (SMAs) are a family of smart materials capable of sustaining large inelastic strains, depending on prior loading history, that can be recovered by heating or unloading. The composition of SMAs significantly influences their mechanical performance: the iron-based and copper-based SMAs are known as lowcost candidates, but their applications are limited by their instability and poor thermomechanical performance (Lagoudas, 2008). The Ni-Ti based SMAs are the most conventional SMA materials and appealed by engineers much more than other SMAs, thanks to their outstanding mechanical properties. SMAs can exist in two distinct phases with three different crystal structures[3] and therefore different properties (see figure 3). The former is the high-temperature phase called austenite, and the latter is the low-temperature phase called martensite (Lagoudas, 2008). The difference in crystal structure between these two phases induces changes in the mechanical behaviour. Furthermore, the core of the SME is constituted by a shear lattice dislocation due to thermal or magnetic active phase transformation. The thermal activated SMAs normally exhibit one-way shape memory effect (**OWSME**) (Mohd Jani et al., 2014), which is described as follow:

- Austenite converts to martensite (A→M) (see in figure 3):

[3] twinned martensite, detwinned martensite, and austenite

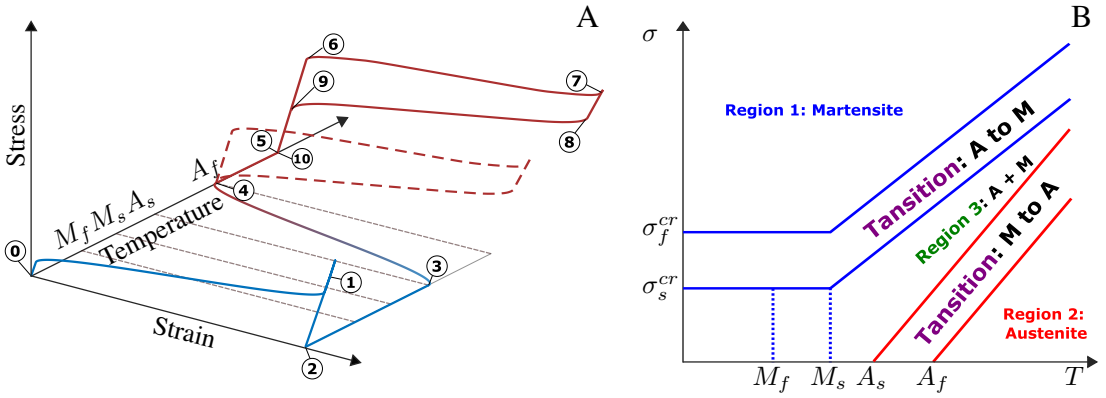

Figure 2. **(A)** An example of modelling of 1D stress-strain-temperature constitutive behaviour of SMA. Shape memory effect: (0) to (4), pseudoelastic loop at constant high temperature: (5) to (10), the hysteretical behaviours are different according to different temperatures. The figure is inspired by (Shaw, 2002). **(B)** An example of Brinson's phase diagram, the figure is inspired by (Brinson, 1993).

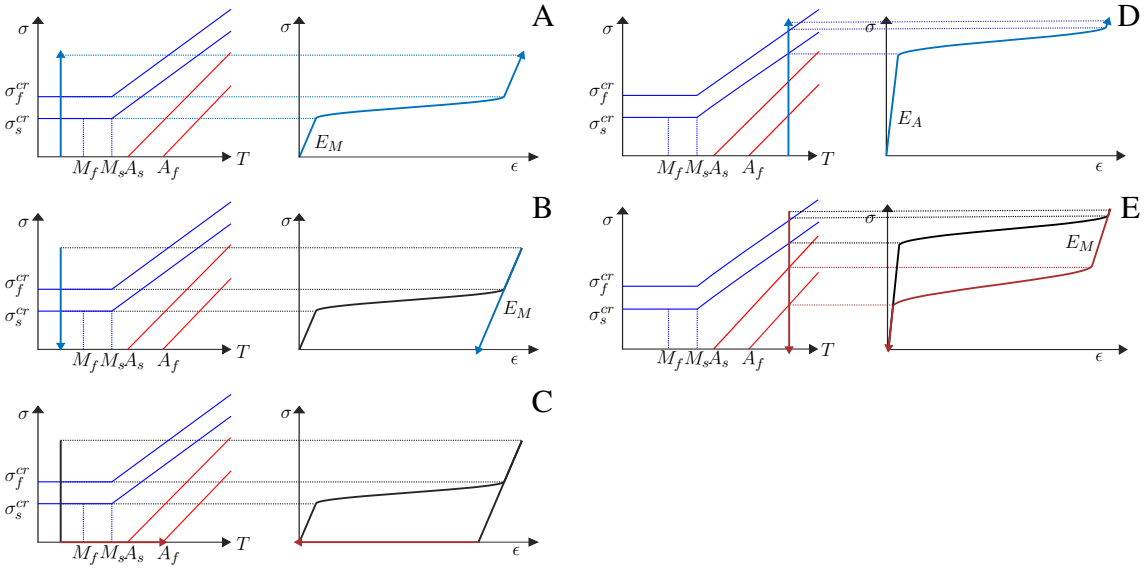

Figure 3. Examples of stress-strain relation of shape memory effect: **(A)**-**(B)**-**(C)** and of pseudoelastic behaviour: **(D)**-**(E)**, the figure is inspired by (Saputo et al., 2020)

1. The A_f signifies the 'austenite-finish-temperature', which corresponds to the end of M→A transformation: the SMA is in a purely austenite state at this temperature. This state is known as the parent state or intial state of SMA.
2. During a stress-free cooling process, the transformation starts to revert from austenite to martensite at M_s 'martensite-start-temperature' and finishes at M_f 'martensite-finish-temperature'. This process induces a formation of twinned martensite phase.
3. When the twinned martensite is subjected to an applied stress larger than the 'critic-start-stress' σ_s^{cr} [4], a reorientation process is initiated, resulting in growth of certain favorably oriented martensitic variants. The reorientation process is finished at the 'critic-finish-stress' σ_f^{cr} (see figure 3A).
4. After the elastic unloading, the detwinned martensitic state is retained with a residual strain ϵ_L (as described in 3B).

[4] σ_s^{cr} is far lower than the permanent plastic yield stress of martensite

- Martensite converts to austenite (M→A) (see figure 3): when the SMA is heated above the 'austenite-start-temperature' A_s , the parent state begins to regain and the strain recovered due to the phase transformation from detwinned martensite to austenite is termed as the transformation strain ϵ^t (see figure 3C).

Subsequent cooling to martensite will again result in the formation of self-accommodated twinned martensitic variants with no associated shape change, and the whole cycle of the OWSME can be repeated (Lagoudas, 2008). M Jani categorised the shape change effect into three shape memory characteristics (Mohd Jani et al., 2014): 1) OWSME, 2) two-way shape memory effect (TWSME) that implies a tendency of the material to undergo mechanical strains with temperature cycling even when it is not pre-strained (Prahlad and Chopra, 2007), and 3) pseudoelasticity (PE)/Superelasticity. The OWSME-based actuators are usually more powerful, reliable and are widely implemented in many engineering applications (Mohd Jani et al., 2014).

2.2 Summary of SMAs' thermomechanical models

This subsection briefly presents the various classes of models available in the literature for describing the behaviour of SMAs. Unlike traditional materials, SMAs show high hysteresis during both M→A and A→M transformations. Physically, these hystereses are dissipation and assimilation of latent heat due to phase transformation that tends to slow down both heating and cooling processes (Velázquez et al., 2006). Consequently, to use SMAs in engineering applications, it is necessary to have an accurate understanding and description of their mechanical behaviour.

2.2.1 Model classification

For years, various constitutive models have been developed by different choices of thermodynamic potentials, internal state variables, and their evolution equations, which provide various insights into the analysis and design of SMA actuators. For example, (Lagoudas, 2008) provides a comprehensive list of 1D and 3D constitutive models with different choices of thermodynamic potentials and internal state variables. As proposed by (Cisse et al., 2016), the models presented here are classified into three categories: microscopic models, micro-macroscopic models, and phenomenological (macro) models.

1. The microscopic models are directly linked to initiation and evolution of multiple martensitic variants upon which superelasticity and shape memory effects are based (Paiva and Savi, 2006). Models in this category are intended to describe microstructural features in SMA behaviour such as phase nucleation (Abeyaratne et al., 1994), interface motion (Duval et al., 2011), martensite twin growth, thus at the lattice or grain-crystal levels. They are useful to understand fundamental behaviour occurring at the microscopic scale, but they are complex to be applied at the device level.
2. Micro-macro approaches combine micromechanics and macroscopic continuum mechanics to derive constitutive laws of the material and often give good predictions. The development of micro-macro models requires the use of suitable observable variables and internal variables. The former usually consist in temperature T and external stress σ or strain ϵ. The latter usually comprise the volume fraction ξ of martensite and a mean transformation strain (Cisse et al., 2016). Fremond (1987) developed one of the earliest constitutive models for SMAs using internal variables. However, these models require very high computational cost, making them difficult to use for the design of engineering applications (Zhu et al., 2013).

3. Phenomenological models (Macroscopic models) are considered as a simplified version of micro-macro models. They describe average material behaviour at macro-scale of SMA components using a limited number of internal variables (for example, only one internal variable like ξ[5] or two internal variables like ξ_T, ξ_S[6]) by assuming the homogeneity and isotropy of material. In general, they are suitable to be used within numerical methods (such as the finite element method - FEM) in an efficient way to predict the effective behaviour on the scale of millimeters to meters (Zhu et al., 2013; Elahinia, 2016).

The reader is referred to the works by (Lagoudas, 2008; Cisse et al., 2016) for more details on the models.

2.2.2 Approaches on phenomenological models

As mentioned previously, the phenomenological models are the most popular models in literature compares with other approaches (Paiva and Savi, 2006), since they avoid to use difficult-to-measure parameters such as free energy and use only clearly defined engineering material constants. Consequently, this approach plays an important role for SMAs-based engineering within SMA's behaviour modelling context. In the literature, Lagoudas (2008) had implicated four critical aspects of characteristic modeling of SMA materials, such as: 1) the phase transformation kinematics, the hardening during phase transformations, and induced SME and PE behaviour (see figure 3); 2) the detwinning of martensite at low temperature, associated to the asymmetric response that SMAs exhibit in tension and compression; 3) the TWSME and the effects of reorientation; 4) the accumulation of plastic strains during cyclic loading. In this paper it is also claimed that the 1D constitutive model is acceptable for tensile and torsional applications such as SMA wires, rods, and tubes, and the statement has been validated experimentally by (Prahlad and Chopra, 2007; Chapman et al., 2011). Recent works on this topic frequently mention the 1D constitutive model developed by Liang & Roger (further for **LRM**) (Liang and Rogers, 1990) and by L.C Brinson (further for **MB**) (Brinson, 1993). These approaches are based on the work of Tanaka (1986) that combines a mechanical and a kinetic law which governs the martensitic fraction of the material (Lobo et al., 2015). Sayyaadi et al. (2012) have compared these models with uni-axial tensile tests and concluded that these three models all agree well in their predictions of the PE of SMAs at high temperatures ($> A_f$). However, the models developed by Tanaka, and Liang & Rogers can not be used for predicting the shape memory effect behaviour with certain initial condition (for example, a residual strain due to a path including detwinning of pure martensite) (Sayyaadi et al., 2012). Besides the reduced-order model, 3D constitutive models using the FEM approach can be found in literature, 'COMSOL' (Collet et al., 2009) and 'ABAQUS' coupling with user subroutine (Zhu et al., 2013; Peraza-Hernandez et al., 2013) are often mentioned in studies. Although accurate and capable, due to the high hysteresis induced behaviour and large strain during phase transition, finite element simulation can lead to a very high computational cost (Barbarino, 2015). However, they are mandatory when complex geometries are involved.

3 SMAS-BASED ACTUATORS FOR TORSIONAL MOTION

SMAs made of NiTi have attracted wide interest in both research and industry due to crystal realignment, which is also the case for torsional motion actuators that are considered in this section, as they require both shape memory effect and high torque output. The performance of SMA actuators is primarily related to their metal composition and geometry. Huang mentioned that for SMA element designing, a trade-off should always be done (Huang, 1998): briefly, straight wires in tension offer small linear motion and high force; torsion bar and tube exhibit large rotation and small torque; cantilever strips for large displacement and small force; helical elements provide large linear motion and small force, or large rotation and small

[5] ξ: the martensite volume factor, 0% presents pure austenitic state, 100% presents pure martensitic state.

[6] ξ_T, ξ_S : the martensite volume factor induced by temperature and the martensite volume factor induced by applied stress.

torque. It is worth to remind that the coil form design offers more design parameters than other simpler geometries. For example, for an SMA torsional coil spring actuator, a common category of actuator, the turns numbers, and diameter of a coil dictate its motion capacity, and the diameter of the wire relates to the output torque. A larger diameter leads to a higher output torque compared to the thinner one. However, beyond their linear actuation in spring or tendon forms, there is little variety research for actuation in torsional motion, which are useful for origami robots. SMA-based elementary actuators can be classified into three categories:

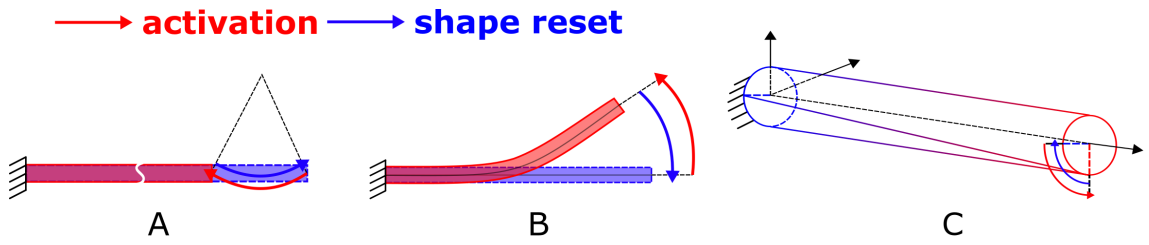

Figure 4. Examples of elementary SMA for uni-directional torsional motion: **(A)** Normal-motion-driven SMA element; **(B)** Bending-motion-driven SMA element; **(C)** Torsional-motion-driven SMA element.

- SMA-based wires and linear springs (see figure 4A): besides other forms of SMA-based actuators, wires are a more common form of actuators (Paik et al., 2010). However, their limited recoverable strain in the range of 4–8% requires them to have lengths up to 25 times longer than their intended stroke length (Rodrigue et al., 2017). A common way to increase output stroke without enlarging an actuator's dimensions is to wind SMA wires around a cylindrical surface, resulting in a coil form actuator. The design consists in accumulating the normal deformation of the wire to global shear deformation of actuator in a single-coil form (**?**) or double coil form (Kim et al., 2015b). In literature, novel arrangements and compliant mechanisms can be found to convert elementary linear strain to global torsional motion. For example, a tensile strain of two SMA wires in two sides of an elastic band can generate a bending motion globally (Wang et al., 2008); an arrangement at constant and opposite eccentricity in a polymer matrix can convert the linear motion into a global twisting of the whole device (Rodrigue et al., 2015a). Rodrigue et al. (2017) had presented an overview of actuators and robots coupled with wire or linear spring elements. In this work it is concluded that the optimization of actuators' configuration for increasing their deformation range is the major challenge according to the structure size and the implementation of power source. As proposed by Paik et al. (2010), the actuators must be small enough to be embedded within the substrate material while sufficiently powerful to achieve folding. These characteristics make the integration of wire elements for self-folding structure a challenging engineering issue.
- SMA-based bending elements (see in figure 4B): SMA bending actuators have been developed for robotics (Hawkes et al., 2010; Paik et al., 2010; Paik and Wood, 2012; Paik et al., 2012; Zhakypov et al., 2016; Firouzeh and Paik, 2015) and medical applications (Sheng and Desai, 2015; Sheng et al., 2017; Abadie et al., 2002, 2009) for years, due to their small form factors, convenience in actuation, and compatibility with medical imaging. Large residual tensile and compression strains are locally distributed on the two sides of actuators in order to generate the torsional motion due to SME. Designs of bending-based actuators can globally be divided into two categories: 1) bending sheet: thin pre-annealed sheets are frequently mentioned in literature as an alternative to mechanical joints. The deformation occurs around an axis defined by the structure deformation rather than having

a rotation between two separate elements, and there could also be some deformation of the structure surrounding the rotation axis (Peraza-Hernandez et al., 2014; Rodrigue et al., 2017). Hawkes et al. (2010) introduced a self-deployable origami structure using a universal crease with triangular module firm. $100\mu m$ thickness pre-annealed sheet elements were integrated at folding creases. The prototypes were proven capable of realizing a '2D→3D' shape changing: a flat sheet maneuvers to fold towards complex shapes such as an airplane or a boat and maintain its shape using embedded magnets. However, the design is limited by the SMAs material properties. It was shown that deformation of a U-shaped metal sheet to its initial flatform is not possible (Firouzeh et al., 2013), because of the plastic deformation of the material that forms a curvature at the hinge. A solution consists in introducing extra curvature to achieve a larger rotation angle. Consequently, additional machining processes such as laser cutting and SMAs layer's pre-annealing are necessary (Paik et al., 2010; Zhakypov et al., 2016). 2) bending wire or cantilever: single or group of linear and arc-shaped SMA wires that are arranged to provide bending motion (Shin et al., 2016). Investigations on SMA-based bending beams and cantilever are carried out for applications that require larger output torque (Abadie et al., 2009; Wang et al., 2016).

- SMA-based torsional elements (see figure 4C): since the conversion between linear motion and torsional motion requires supplementary mechanisms, resulting in energy dissipation (friction, extra mass) and operation space requirement, studies on SMA-based torsional elements have been developed in the last decade. Using this type of design, large recoverable shear deformation [7] can be obtained simply by gripping both ends without any extra mechanism. Consequently, the fabrication and assembly process can be simplified. Different designs of elementary torsional actuators can be found in literature, rotary actuation capability are experimentally proven using torsional strips (Tobushi et al., 2008, 2010, 2013), torsional bands (Shim et al., 2015), torsional wires (Kim et al., 2015a) and torsional tubes (Benafan et al., 2019). Besides the shear-strain-driven-actuators, investigations on torsional coil spring (Salerno et al., 2013; Sheng and Desai, 2015; Sheng et al., 2017) that convert the local normal strain to global shear strain are carried out and results show an improvement of motion range and reduction of output torque compared to the wire form torsional actuator. It is worth reminding the works introduced by Kim et al. (2015a) and by Wood et al. (2016), that presented the origami-based self-deployable structure coupled with torsional wire elements. The former was based on a 'Kresling' pattern, and the latter was based on a 'Waterbomb' pattern. Prototypes showed a global shape morphing driven by torsional actuation at folding creases with more than 90 degrees rotation. Additionally, interesting structural performance such as 'buckling effect' due to pattern design were observed Kim et al. (2015a). However, these structures required external force to be re-folded after activation.

To sum up, normal-strain-driven actuators offer different advantages such as simplicity of manufacturing, simplicity of multi-physical modelling, suitable for conventional cooling. However, the requirement of operational space and complexity of supplementary mechanism limits the capacity of this design. Bending-elements offer the same level of motion and allow the possibility of size reduction of actuators but require supplementary fabrication. Torsional elements have shown an interesting potential due to their larger angular motion-range and larger output torque within a limited space. Regarding origami-inspired structures, which require large torsional actuation within very limited operational space (Hawkes et al., 2010) at folding creases, these characteristics makes them an appropriate candidates for origami-inspired robotics (Koh et al., 2014; Kim et al., 2015a).

[7] compared to a conventional torsional strain-based application, such as SMA linear springs (An et al., 2012)

4 ACTUATORS FOR BI-DIRECTIONAL TORSIONAL MOTION

Conventional SMAs can only achieve unidirectional actuation, thus it is necessary to provide an external force to carry out a repeatable bi-directional motion. According to the nature of this force, two classes of SMA actuators can be defined: passive bias type SMAs actuator and active bias type SMA actuator (Georges et al., 2013). The former one, composed of an SMA element and a bias load (constant mass, linear or nonlinear stiffness spring), offers the simplicity of modelling and manufacturing but its performance (dynamic response and motion range) is highly dependent on the choice of passive element. The latter one, which consists of two antagonistic SMA elements, has faster speed of response than the former one, but it requires more power (Khan et al., 2016) and the output torque is restricted by the stiffness of the antagonistic components. These two categories are described in the following. Table 2 provides an overveiw of the principles, dimensions, performance, heating and cooling strategies, models used for design and controlling issues for a large number of SMA-based BTM actuators.

4.1 Passive biased actuator

As reminded before, an SMA-based actuator should first be pre-deformed at low temperature ($< M_s$) and then activated to a higher temperature ($> A_s$) to initiate its controlled contraction due to the M→A transformation. This controlled contraction can then be used to generate mechanical work. Passive elastic

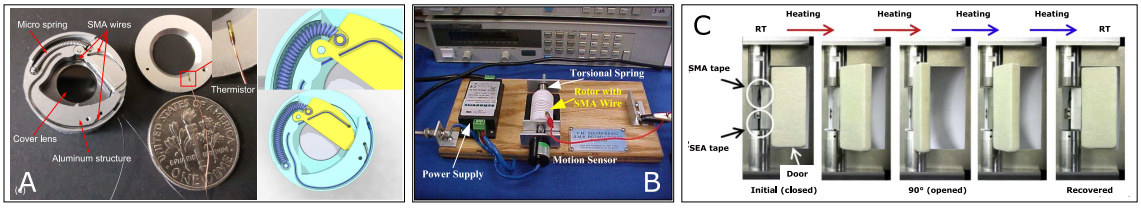

Figure 5. Examples of BTM actuator using SMA wire element: **(A)** A mesoscale SMA actuator for cleaning the contaminated lenses of surgical cameras during minimally invasive robotic surgery (Liu et al., 2019); **(B)** A rotary servo driven by a coil form SMA wire, the shape 're-set' torque is provided by a torsional spring (Song, 2007); **(C)** An opening and closing door device capable of a two-way rotary motions using a combination of a SMA & SEA(superelastic alloy). The strip was biased passively by a PE behaviour element for position resting (Tobushi et al., 2013).

elements have been widely used in SMA-coupled innovations since they are simple to be engineered and integrated into structures. Although, beyond the utilization of traditional springs, elastic or super-elastic elements can take the place of springs to achieve specific requirements, such as reducing working space or amplifying rotation stroke. However, the spring force is passive and decreases as the pulley moves back to the original position. Without high initial tension, residual displacement is unavoidable (Lan et al., 2009). Jenkins and Landis (1995) presented an SMA-actuated rotating arm for moving the cover glass of a solar cell on NASA's Mars Pathfinder using a wire actuator with 0.15mm diameter activated with Joule-effect heating. A similar design at a miniature scale has been implemented by Liu et al. (2019) (see figure 5A) for medical applications, by Khan et al. (2016) for robotics applications and Basaeri et al. (2014) for aeronautic applications. Design with coil form torsional SMAs with passive spring are studied in (Lucy and Center., 1996; Redmond et al., 2010; Song, 2007) (see figure 5B); shear strain-driven actuators are presented in (Tobushi et al., 2010; Takeda et al., 2012; Prahlad and Chopra, 2007; Chapman et al., 2011). Besides the utilization of conventional springs with linear stiffness, functional materials such as pseudo-elastic SMA or PDMS(Yuan et al., 2017a) with visco-elastic behaviour are introduced to improve the rotation stroke while resetting the actuator's pre-strained state. For example, Yuan et al. (Yuan et al., 2017a) introduced a helical spire form rotary actuator driven by linear SMA wire. The 're-arm' force being generated by structural

stiffness made by Acrylonitrile Butadiene Styrene (ABS). Takeda et al. (2012) presented two-way rotary motions of an opening and closing door device (see figure 5C) and a solar-powered active blind model driven by a SME-based twisting strip. The strip was biased passively by a PE behaviour element for to reset position. The rotation modular was shown capable of rotating of 45 degrees with fatigue life longer than 3×10^6 cycles. One needs to remind that these constant stiffness elements are frequently used to characterize SMA's performance (Prahlad and Chopra, 2007; Chapman et al., 2011; An et al., 2012), which somehow constitutes a passive biased actuator.

4.2 Active biased actuator

The passive bias components discussed above require fine tuning to cooperate correctly with the actuator. Instead of using passive bias elements to 're-arm' the actuator, integrating active bias elements such as an antagonistic SMA element is a very efficient way to create devices capable of producing differential motion paths and two-way motion (Georges et al., 2012). The current rotary actuators using this design can be classified based on their actuation elements, which we have previously described in Section 3.

4.2.1 Linear SMA element with mechanical joint

This design consists in converting the linear contraction strain of the SMA element to torsional motion using a mechanical articulation such as a pulley or a compliant joint, thus creating a torque about this joint on contraction, where the torque arm is the distance between the SMA wire and center point of the joint (Rodrigue et al., 2017). Consequently, design parameters are the structure geometry and also the dimension of the SMA wire. For example, in their work, Kirsch et al. (2020) shown an actuation system consisted of an antagonist wire element of 0.025mm diameter and 550mm length and a pulley of 3mm in diameter. The SMAs are heated using the Joule effect and cooled using natural air convection, resulting in a rotation stroke of 31 degrees with an actuation frequency of 10Hz. Doroudchi et al. (2018) used the

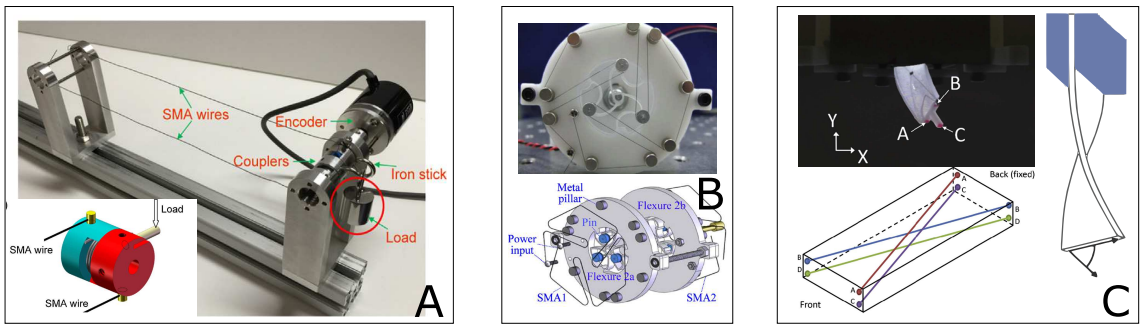

Figure 6. Examples of BTM actuator using SMA wire element: **(A)** A rotary modular using 'antagonistic Linear SMA + pulley' design with a intermediary torsional spring (Guo et al., 2015); **(B)** A rotary modular using 'antagonistic Linear SMA + optimized spring-slack element + pulley' design with compact arrangement of linear SMA (Lan et al., 2009); **(C)** A BTM actuator consists of four SMA wires embedded in a soft matrix. The actuator is capable of performing banding and twisting motion in two opposite directions (Rodrigue et al., 2015b).

same design and a similar length for the SMAs but a 20mm diameter pulley. The actuator provides only 1 degree of stroke with the same frequency, using only forced air convection. Based on this typical design, various contributions can be found in literature: 1) supplementary mechanism or complex design to amplify the rotary stroke; 2) advanced controlling model for the accuracy of rotary system; 3) enhanced heating or cooling method for improvement of response dynamic; Focusing on the first improvement, Guo et al. (2013, 2015) introduced a bi-directional rotary actuator with a torsional intermediary compliant spring, and the stroke was amplified from 10 degrees to 30 degrees (see figure 6A). V. Bundhoo and G. Gilardi

(Bundhoo et al., 2009; Gilardi et al., 2010) developed a tendon-driven actuation system for artificial fingers with a complicated feedback control system, the antagonist SMAs are both embedded with a spring and a stopper to amplify the stroke up to 80 degrees. Based on this approach, Lan et al. (2009) developed a BTM actuator equipped with a pair of SMA wires with a compact arrangement and an optimized structural contractive part (see figure 6B). The actuator has proven ability of a 14 degrees angular stroke. Nespoli et al. (2010) introduced a meso-scale rotary modular using two wire elements. The wire elements are pre-annealed into flat spring to achieve a compact design, the prototype shown its capability of offering a rotation stroke of 160 degrees corresponding to 4.5mm displacement in opposite directions. Concerning the second improvement, Moallem and Tabrizi (2008) introduced a detailed multi-physics 1D model, which firstly used a LRM based differential form martensite factor. The BTM actuation prototype has be proven capable of 20 degrees stroke rotation with a maximum error of 0.5 degrees using motion feedback. Based on this approach, Moghadam et al. (2019) showed that the introduction of BM and a cascade control offers better accuracy than the former. Ruth et al. (2015) proposed a self-sensing actuator using electrical resistance measurement, and the prototype showed a result of a 30 degrees stroke with a 2 degrees error. For the third improvement, the work of Doroudchi et al. (2018) used forced air convection to accelerate the cooling time, resulting in 5Hz with a 4 degrees stroke and 10Hz with a 1 degree stroke. Another method is presented by (Ianagui and Tannuri, 2011). In this work, a Seeback effect-based (Romano and Tannuri, 2009) cooling tablets was introduced. Resulting in a ± 7 degrees motion with a frequency of 1.3 Hz. Beyond the utilization of conventional design, novel architecture of actuators and arrangements provide more possibilities for applications. For example, Rodrigue et al. (2015b) shown an actuator of a rectangular polydimethylsiloxane (PDMS) matrix embedded with two pairs of SMA wires maintaining a constant eccentricity from the middle plane across the thickness (see figure 6C). The prototypes have been proven to offer both bending and rotating motion using Joule effect heating. Koh and Cho (2013) have introduced an inchworm-inspired origami-based climbing robot using a single SMA spring in the body and use flexible hinges actuated by antagonistic SMA springs in the legs with anisotropic friction pads. Zhakypov et al. (2015) presented a low profile centimeter-scale origami robot actuated by three antagonistic SMA linear springs. The 4g weight robot is capable of jumping as high as five times its height. De Sars et al. (2010) developed a multi DOFs structure actuated by thin waveform NiTi layer springs mounted in an antagonist configuration and directly integrated into the structure of an endoscope.

4.2.2 SMA-based flexural joint

Besides the linear SMA, bending-strain-driven SMA-based actuators are also mentioned in literature. This design is an alternative to mechanical joints. Instead of transforming linear motion to rotation, a hinge-like joints using reversible bending material at the rotation axes is carried out in order to achieve the bi-directional actuation. In literature, this kind of design is usually referred to as 'flexural joint' (Peraza-Hernandez et al., 2014; Rodrigue et al., 2017). Paik's and coworkers presented several researches on Origami robot coupling with SMA-based actuation in bending layer form (Paik et al., 2010; Paik et al., 2011; Paik et al., 2012; Paik and Wood, 2012; Firouzeh and Paik, 2015; Zhakypov et al., 2016). The pre-annealed thin sheets form SMAs are generally mentioned as the elementary actuators. Based on this design, different contributions were carried out: the actuator was first presented in 2010 (Paik et al., 2010) using a sheet of $500\mu m$ in thickness with fabrication process, an analysis of the designing of external heater was also addressed, and an experimental test bench is introduced. The actuator was demonstrated capable of rotating with 180 degrees. A 'print-on' stretchable electrical circuit was then studied to achieve the sensing and controlling of this miniature self-folding based actuator (Paik et al., 2011). The design was further improved using a novel arrangement (Paik and Wood, 2012), an 'S' form pre-annealed sheet actuator coupled with a Joule effect based flexible heater was presented. The results have shown a capability

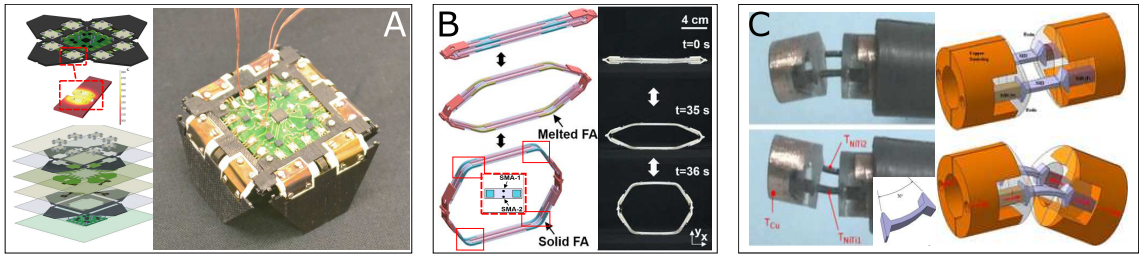

Figure 7. Examples of BTM actuator using SMA bending element: **(A)** A prototype of 'Robogamis', a two-dof local motion robot using four pairs of thin-layer-form antagonistic SMA (Firouzeh and Paik, 2015); **(B)** A self-deployable structure with four hinge-like joints for BTM, four pairs of antagonistic thin-bending-rod form SMAs have been embedded (Wang et al., 2016); **(C)** A prototype of torsional micro-actuator for active endoscopy application with a pair of antagonistic bending cantilever form SMAs. A Peltier-effect-based heater & cooler has been integrated (Abadie et al., 2009).

of a 180 degrees rotation in opposite directions. Zhakypov et al. presented a complete study including modeling-based designing, sensing, and controlling the actuator (Zhakypov et al., 2016). The actuator was further embedded with 1 SMA spring with two flexible articulations in the middle to realize a 'clamp - jump' motion (Zhakypov and Paik, 2018). Firouzeh and Paik (2015) presented a four-legged origami robot named 'Robogami Crawler' that is capable of providing locomotion with 2 dofs using four folding modules. Each module consists of a pair of flat 2D SMA with $100\mu m$ thickness sheets in antagonist configuration (see figure 7A). Elementary SMA was proven to rotate with a maximum angle of 120 degrees with 5-16mNm [8] output torque. The antagonist pair are proven of providing a $\pm$ 60 degrees motion while providing 0.83 mNm torque to overcome the friction. Apart from works of Paik's group, Gilpin et al. (2014) developed a Hexroller shape close chain combined with a series of personalized bending SMA layers is developed in order to realize locomotion in one dimension. Abadie et al. (2002) presented a micro-actuator called 'Ω modular' with a Ω form bending strip. One need to highlight that he first used Peltier effect and Thompson effect to accelerate the thermal exchanging process. Abadie et al. (2009) further enhanced this design with a pair of bending cantilever and a thermoelectric temperature controller for active endoscopy applications (see figure 7C). Beyond the sheet form geometry, other conceptions such as bending wires, bending strips, and bending cantilevers have been investigated. Since the maximum strain of SMA for cyclic applications is limited to 3% - 4%, single bending elements usually offer relatively lower stroke than other designs. Thus the actuation system often arranges the bidirectional SMA elements in series or in parallel to achieve either a larger stroke or a higher output torque globally. Kuribayashi (1989) presented a millimeter-sized actuator using two pairs of thin bending SMA strips. The prototype can provide a stroke of ± 80 degrees with an output torque of 0.04mNm. Wang et al. (2016) introduced a 'hinge-like' BTM actuation modular consisted of 0.15mm diameter and 15mm actuation length (190mm of total length) antagonist bending wires embedded into a PDMS elastomer matrix. The modular was proven capable of providing a BTM 90 degrees rotation and of blocking its shape[9] using a thermal-controllable stiffness joint made of fusible metal[10] (see figure 7B). Kim et al. (2019) developed an actuator to provide angular displacements in both clockwise and counter-clockwise directions with compliance using 28 pairs of bending wires in parallel in opposing way. Roudaut et al. (2013) proposed novel display conceptions for mobile devices that can morph their shape using SMA actuation driven by an SMA composite with a mesh of bending SMA wire.

[8] these two values are according to the begin and the finish state of 'M$\rightarrow$A' transition

[9] to maintain the desired shape without additional force after actuation

[10] a 32.5%Bi, 16.5%Ti, 51%In that can be melt at relatively low temperature while avoiding the degradation of device, the material is heated by a commercial Ni-chrome wires

Wang et al. (2008) developed an embedded SMA wire actuated biomimetic fin for underwater propulsion. A micro-robot fish (146 mm in length, 30 g in weight) using antagonistic SMA wire with a silicon-based elastic substrate are shown as a prototype, this actuator can achieve a rotation angle of ± 90 degrees.

4.2.3 SMA-based torsional joint

As already mentioned, twisting deformation based elements offer several benefits such as design simplicity and large shear strain. However, comparing other forms of actuators, the research on bi-directional actuation using twisting elements is very limited. Sheng and Desai (2015); Sheng et al. (2017) introduced a torsional

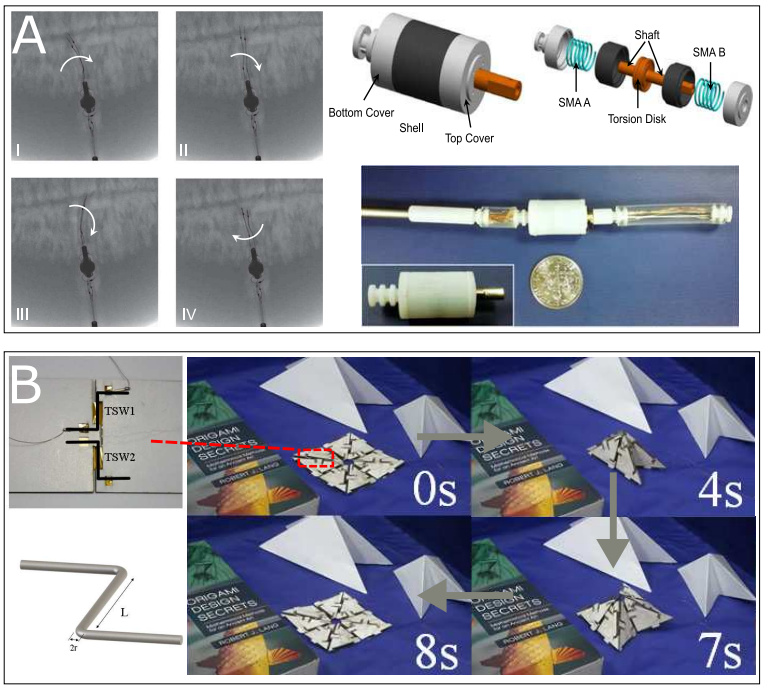

Figure 8. Examples of BTM actuator using SMA torsional element: **(A)** A meso-scale BTM modular embedded 2 antagonist torsional springs for surgical application (Sheng et al., 2017); **(B)** A meso-scale self-deployable paper-based open origami structure that capable of switching between 2D-3D state(Koh et al., 2014).

actuator using torsional spring in antagonist configuration for a surgical robot prototype to demonstrate its working performance in humid environment under C-Arm CT image guidance. The study shown a rotation stroke of ± 20 degrees at 0.05 Hz (see figure 8A). Koh et al. (2014) introduced a torsional SMA wire actuator embedded in patterned origami structures. The wires of 0.4mm in diameter and 12mm in length were pre-twisted at 360 degree in opposite direction for each and resulting in achieving a typical origami 3D-flat transition within 4s using applied current of 0.8A (see figure 8B). Based on this approach, Kim et al. (2016) presented a shape-shifting system consists of distributed self-deployable origami modules using a modified bi-stable 'Kresling' pattern. Two pairs of antagonist $250\mu m$ diameter and 8 mm length torsional wire were embedded on each module. The prototype was proven capable of switching the shape driven by 90 degrees BTM actuation at folding creases with 1A for 5 seconds. One needs to highlight that the system was capable of shape-blocking thanks to structural bi-stability due to the origami pattern. Similar design of actuation system in large scale were investigated in aeronautic domain, Benafan et al. (2019) developed bi-directional torsion actuator using antagonist SMA tube for NASA's the spanwise adaptive wing (SAW) project. The SMA tube has 3mm thickness and 304mm in length, resulting by a folding motion of ± 70 degree of wings during a flight test .

5 DISCUSSION

This section introduces a discussion on critical topics related to SMA actuators. The characteristics discussed here are the available analytical tools for describing actuators' behaviour, performance prediction and designing driven by inverse model, the temperature controlling strategies, sensing, and position/force control.

5.1 Analytical tools for bi-directional SMA actuators

As mentioned in section 2.2, SMAs' high hysterical behaviour usually depends on their temperature history and applied stress. Consequently, a reliable model becomes necessary for the actuator design. The discussion about bi-directional SMA actuators is divided in two parts : (1) thermal modelling for the computation of the temperature distribution; (2) thermomechanical modelling for prediction of the motion range and actuation torque.

5.1.1 Electro-thermal model

Since the SMAs mechanical behaviour depends on the thermal evolution path, it is necessary to describe the temperature distribution of SMAs. For most of bi-directional actuation, the geometry of SMA element is usually straightforward. Hence 1D thermal balance modelling can be used by assuming the uniformity of temperature distribution T with Biot condition B (Shahin et al., 1994), such as:

$$\rho V \left(C\frac{dT}{dt} + \Delta H \frac{d\xi}{dt} \right) = \phi_s - \phi_{\text{dissipation}} = I^2 R - hS(T - T_{amb}) \tag{1}$$

$$B = \frac{hl}{\lambda} < 0.01 \tag{2}$$

where $\phi_s, \phi_{\text{dissipation}}, \Delta H, C, h, \rho, \lambda, S, V, l, \xi, I, R, T_{amb}$ the thermal source flux, the thermal dissipation flux, latent heat rely to the phase transition of SMA, the thermal capacity, the thermal conductivity density, the convective heat transfer coefficient, the surface area of the SMA wire of actuator, the actuator's volume, activation length, the martensite factor, the input current, the electrical resistance and the temperature of the surroundings, respectively. The equation corresponds to the typical case (see table 2) with Joule effect heating and natural air convection which is a very common use of SMAs-based actuators. The partial differential equation can be implemented easily in order to realize a real-time modelling of actuator thermal behvaiour. Moreover, Abadie's model (Abadie, 2000) utilized the same method but the differential element corresponds to Peltier effect and Paik and Wood (2012) have used 3D FEM approach to predict the temperature distribution for cantilever or thin sheet elements. Additionally, the dissipation term can be modified to meet different cooling methods, such as forced air convection (Doroudchi et al., 2018), water or oil based convection(Wang et al., 2008) and thermal conduction or thermo-electrical effect based dissipation method (Shahin et al., 1994; Abadie, 2000; Romano and Tannuri, 2009). In literature, investigation on the change due to thermal convection coefficient and electrical resistance are carried out to improve the models' performance. Shahin et al. (1994) introduced a complex formulation to estimate the air convection coefficient, and he offered a simpler expression using typical values for air properties:

$$h(T) = -0.379 + 20.563 \log_{10}(T) \tag{3}$$

One need to remind that for certain case like thin linear SMAs wires, the variation of electrical resistance of actuator can show a non linear behaviour due to phase transition and shape changing (Ruth et al., 2015). Such investigation is presented in Velázquez et al. (2006), in which he developped a temperature and deformation based function of electrical resistance, resulting in improvement of modelling precision.

The influence of latent heat is another factor that has been usually neglected for mathematical simplicity (Moallem and Tabrizi, 2008; Guo et al., 2015; Moghadam et al., 2019; Liu et al., 2019; Peraza-Hernandez et al., 2014). Beside the utilization of reduced order model, the numerical approach using 3D FEM method are presented in literature in order to study the temperature evolution more accurately (Abadie et al., 2009; Paik and Wood, 2012; Firouzeh and Paik, 2015). For example, Paik and Wood (2012) shown a local heating effect due to personalized heater to optimize energy efficiency using FEM. However, these models provided only the prediction of thermal behaviour without coupling mechanical hysteresis of SMAs.

5.1.2 Thermomechanical modeling of actuator for BTM

As mentioned in Section 2.2, 1D quasistatic phenomenological models implemented in numerical softwares are frequently utilized to predict the thermomechanical response of actuators. The LRM/MB are demonstrated as a suitable model for prediction of the quasistatic and dynamic response of passive or active biased normal stress actuator for BTM (Liu et al., 2019; Moghadam et al., 2019; Doroudchi et al., 2018; Gilardi et al., 2010) . Moallem and Tabrizi (2008) introduced the rate of martensite factor evolution based on LRM for dynamic response prediction. Based on this approach, Moghadam et al. (2019) shown an improvement of precision of controlling using a modified version of MB. Additionally, the LRM model is validated experimentally using antagonistic SMA torsional spring in (Sheng et al., 2017). It is worth reminding that Liang and Roger's hardening function are given as,

$$\begin{aligned} M \rightarrow A: \quad & \xi = \tfrac{\xi_M}{2}\left\{\cos\left[\tfrac{\pi}{A_f - A_s}(T - A_s - \tfrac{\sigma}{C_A})\right] + 1\right\} \\ & \text{for } A_s + \tfrac{\sigma}{C_A} \leq T \leq A_f + \tfrac{\sigma}{C_A} \\ A \rightarrow M: \quad & \xi = \tfrac{1-\xi_A}{2}\cos\left[\tfrac{\pi}{M_s - M_s}(T - M_f - \tfrac{\sigma}{C_M})\right] + \tfrac{1+\xi_A}{2} \\ & \text{for } M_s + \tfrac{\sigma}{C_M} \leq T \leq M_f + \tfrac{\sigma}{C_M} \end{aligned} \tag{4}$$

with ξ_M, ξ_A, C_A, C_M the initial values of martensite factor for each transformation process, the material constants that indicate the influence of stress on the transition temperatures, respectively (Liang and Rogers, 1990). A simpler formulation is frequently mentioned in literature concluded that it is acceptable for motion prediction (Rodrigue et al., 2017; Zhakypov et al., 2016; Liu et al., 2019; Shahin et al., 1994) by replacing the initial value ξ_M and ξ_A by a scalar value 1, that assuming every actuation cycle begin with a 100% phase transition. Facing others forms of actuator, the capability of the reduced-order model is proven according to certain designs. Based on the study of Zhakypov et al. (2016), the LRM is proven acceptable for pre-annealed thin SMA sheet with a curvature by assuming pure bending since the curvature length is much larger than the layer's thickness. The Lexcellent 1D model was implemented in Abadie et al. (2002) and Paik and Wood (2012) using stack of thin layers assumption for bending cantilever and bending sheets form actuator. However, only tensile behaviour was considered in these models. For shear-stress-driven elements, LRM/BM based modelling are proven available for linear SMA spring (An et al., 2012; Velázquez et al., 2006). However, for works rely on large-shear-strain-driven SMA elements such as torsional wires, strips, rods, and tubes, full study on actuator multi-physical modelling can not be found in the literature. Available researches focusing on modelling of thermomechanical behaviour are given as follow: for reduced order phenomenological model, exact solution based on BM and Lagoudas models can be found in works presented by Prahlad and Chopra (2007), Chung et al. (2006) and Mirzaeifar et al. (2010). A reduced-order mechanical model is given

$$\gamma = \frac{\theta r}{L} \tag{5}$$

$$\tau = \frac{Mr}{J} \tag{6}$$

$$J = \frac{\pi r^4}{2} \text{ for rods, } J = \frac{\pi}{2}(r_{outer}^4 - r_{inner}^4) \text{ for tubes} \tag{7}$$

with γ, τ, θ, M, J, r, L the shear strain, shear stress, rotation angle, subjected torque, polar second moment, radius and length of actuator, respectively. Experimental data of torsional SMA elements can be found in (Prahlad and Chopra, 2007; Chapman et al., 2011; Doaré et al., 2012; Rao et al., 2014) , the results shown that reduced order models combined with equation 5 to 7 sufficiently predicts the behaviour of thin-walled tubes and thin rod/wire with diameter up to 6mm. A 3D FEM model offers more accurate results for thick wall tubes or thick rods. Work by Zhu et al. (2013) shown that results are given based on Lagoudas, Brinson and Auricchio model in 3D FEM framework yield similar global torque-angle relation for pure torsional motion for a tube of 20mm in diameter and 1.5mm in thickness (see in figure 9A). Figure 9B shows simulation results of 3D FEM model and experimental data of PE behaviour of three SMA torsional wires with the same length and different diameters around 0.5mm provided in work by Chapman et al. (2011). The results show that the 3D FEM model can accurately capture the influence of design parameters on global response with a high hysteresis. Besides the analytical approach, the stress-strain experimental data can also be used for the prediction of actuator performance (Firouzeh et al., 2013; Zhakypov et al., 2017). To sum up, for multiphysics modelling of active bias actuators, currently, the most popular strategy

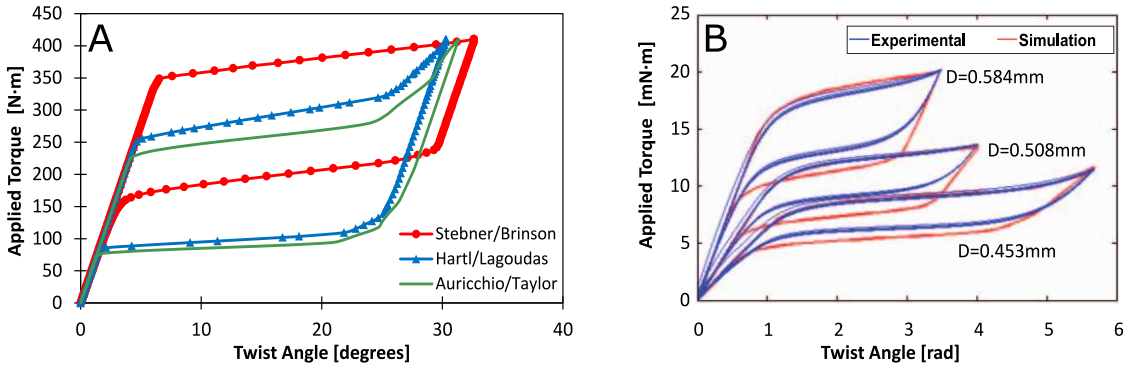

Figure 9. An example of simulation results with 3D FEM frameworks for pure torsional SMA elements: (A) Torsional PE behaviour of a centimetre-size SMA tube form actuator for different models (Abaqus) (Zhu et al., 2013) (B) Torsional PE behaviour of millimetre-size SMA wire form actuators for different diameters (Abaqus), the figure is reproduced from (Chapman et al., 2011)

is directly using the existing 1D models, like the classical LRM or BM coupled with thermal balance equation (see table 2). So far, this approach has led to interesting results. However, it does not fully describe the response for more complex geometries such as bending sheet and torsional elements. As mentioned in section 4.2.3, the existing applications demonstrated active bias torsional elements' capacity, but complete modeling of its nonlinear response is still on demand.

5.2 Actuators characterization

The characterization of actuators is presented in two parts: (1) characterization of elementary SMAs, and (2) characterization of actuation systems. Focusing on elementary SMAs, two tests are frequently mentioned according to model parameters identification and test simplicity: the isobaric test and the isothermal tests. The former is to capture the hysteresis at constant tensile force or torque with cooling-heating cycles. The latter is to capture the PE behaviour with constant high temperature using loading-unloading cycles. With

these tests, the SMAs element's material parameter and performance can be identified. Other tests such as blocked strain test that combine the 'Austenite curve' using different constant strain[11], fatigue test for accumulation of permanent strain during cyclic loading and power consumption tests can be found in literature but will not be discussed in this work. One need to remind that, these tests are normally taking place using wire form simple (Chapman et al., 2011; Prahlad and Chopra, 2007; Doroudchi et al., 2018; Guo et al., 2013), but parameters directly identified from a torsional test are shown to be acceptable for work with unconventional form element (Zhakypov et al., 2016). However, several technical problems need to be addressed due to measurement difficulties. In the work of Churchill et al. (2009), it is indicated that the results of SMA wires tests highly rely on specific factors such as temperature controlling, loading methods and measurement techniques. For example, unlike conventional metals, where temperature variation can be tolerated without influencing the results' accuracy, an SMA wire's response can be significantly affected by a few degrees of change in sample temperature. Thus temperature sensing and controlling for a themo-electrical effect based SMA are very difficult. Such problems will be also validated in the case of torsional elements. Consequently, experimental results of the millimeter-sized torsional elements are minimal than that of centimeter size. Introduction of the phenomena that can lead to testing problems and technical solutions for accurate qualifications are proven to be challenging.

Focusing on BTM actuators, investigations based on two key performances can be found in the literature, such as the motion range and the output torque. The former is relying to the capability of local motion, which is the main objective in robotic and medical domains. The latter is often the mean objectives of works in aerospace and automobile domain. Based on the review, the bending cantilever offers lower stroke than the others design, the 'linear + pulley' design offers maximum rotation angle of 180 degrees but highly depends on pulley's radius and requires large operation space. However, the supplementary mechanism has been frequently mentioned in the literature and has been identified as a source of friction. The antagonistic torsional elements arrangement provides a larger stroke than others designs without any supplementary mechanism (Koh et al., 2014). It is important to mention that, the actuators are attached on a origami-inspired paper-based open structure, thus the output torque has not been characterized. Base on table 2, characterizations are usually focusing on SMA elements performances and system motion range. The strategies and methods for system output torque measurement are still in demand.

5.3 Actuators performance prediction and designing

The SMAs' behaviour importantly depends on its thermomechanical loading path due to its high hysteresis. In fact, since SMAs element usually need an external bias force for re-initialization of shape, the understanding of the stress–strain-temperature dependence becomes extremely important for the choice of design parameters. Generally, the capability due to SME of an SMA according to certain temperature is well described by its 'M→A curve' so-call 'Austenite curve' (see in figure 3(E)), which can be identified and modeled using method described in 5.2. Figure 10 shown a stress-strain relation of a typical actuation system defined by two identical SMA active elements and pre-deformed at the same level. The blue and green curve presents the inelastic behaviour according to pure martensite state and the red curve shows the 'Austenite curve' at a certain high temperature. The figure on the left shown a typical bidirectional actuation configuration, the activated SMA only needs to overcome the reaction of its cooled antagonist component, then finish the activation at the equilibrium point (B), and follow by an elastic release during cooling with a definitive equilibrium as soon as the power is off. Then the strain between (B) and (D) presents the motion range of actuator and the (C) and (E) present the equilibrium point at martensite state. The figure on the

[11] For example, using similar electrical input condition with different blocking position, using measured torque at same time to construct the 'Austenite curve' (Zhakypov et al., 2016)

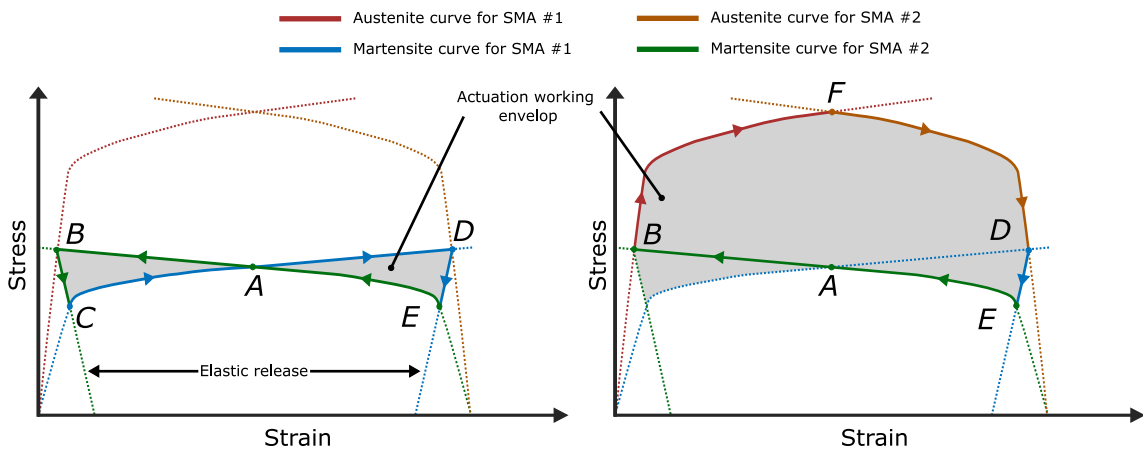

Figure 10. Example of active biased SMA performance tests : left image: motion range tests, the (B-D) presents the maximum of motion range. right image: maximum output stress tests, the F presents the maximum output stress of system at certain temperature. The figure is inspired by (Georges et al., 2012)

right shows the scenario of providing maximum output stress of SMA $\#1$ to conquer the stiffness provided by the activated SMA $\#2$. Using this tool, user can rapidly establish a primary design parameters using experimental data (Firouzeh and Paik, 2015). Additionally, inverse model using identified parameters (for example in figure 9B) can be generally used for determining the design parameters according to application requirements. For example, A non-rigid Kresling-pattern-based origami structure so-call 'Kresling tower' can perform a shape morphing using a global actuation (Jianguo et al., 2016) at the tower's center-line or local actuation at the 'hinge-like' folding creases (Kim et al., 2015a). The former usually requires higher torque to overcome the structural stiffness (Li et al., 2019), and the latter requires a larger rotation angle. Focusing on the inverse model for design parameters of actuation system, certain design constraints should be carefully taken into account in order to avoid the degradation of actuation system. In fact, The SMAs can be damaged with excessive mechanical load or thermal load (Mohd Jani et al., 2014). Many researchers have concluded that thermal load is an important factor of determination of Ni-Ti based SMAs' fatigue performance. Overheating reduces significantly the fatigue life of SMA actuators (Mohd Jani et al., 2014) and damage the structural material. To ensure the applications are intended to perform securely over countless cycles (around 10^6 cycles), the condition such as maximum function temperature, the maximum strain (Huang, 2002; Dynalloy, 2011) and the safe design load (Reynaerts and Van Brussel, 1998) should be carefully decided and consequently utilized as the feasible domain of optimization of design parameters.

5.4 Activation and cooling strategies

The heating and cooling path is an essential requirement for SMAs' mechanical response. The former relies on the SMA activation due to the 'M→A' transition, and the latter relies the 're-arm' process of actuators. In fact, low speed response and low energy efficiency are two of the main SMA disadvantages (Mohd Jani et al., 2014; Paik et al., 2011; Doroudchi et al., 2018). Various thermal power supplying and removal methods can be found to this end. Concerning SMAs activation, strategies are given as:
1) Joule effect heating using the actuator body as the resistance in the electrical circuit. Consequently, higher current offers higher activation speed. In fact, this method is proven as the best method for low-diameter normal-stress-driven SMA because of its simplicity and controllability. However, high current can cause problems for associated electrical traces due to I^2R losses, where I and R are the current and electrical resistance, respectively.

2) External heater-cooler using thermoelectric effect such as the Peltier effect, the Thomson effect and Seeback effect.(Abadie et al., 2002; Shahin et al., 1994) The electrical current applied to the module is able to heat or cool the SMA element of the actuator. Studies based on this method are presented in (Abadie et al., 2002, 2009). An SMA blade-form actuator realized by a thermoelectric system composed of two bismuth telluride (Bi_2Te_3) ingots is tested, resulting by an improvement of response dynamic during cooling. The figure 11 shows a guideline to determinate the activation method.
3) External heater using thermal conduction often consists of resistance wire or thin layer. This method offers a solution to overcome the low electrical resistance due to actuators design and SMAs' material properties. Works presented by Paik offer an analysis focusing on designing of an external heater made of Ni-Cr alloy (as called 'Inconel') with different forms, such as a coil form wire heater (Paik et al., 2010), or a thin-film layer form with 2D pattern heater (Zhakypov et al., 2016; Paik et al., 2012). The results shown that this Ni-Cr heater offers a 20% reduction on response time and around 53% reduction of power consumption than Joule-effect-based heater. To sum up, the Joule effect-based heating is proven a common method for SMA activation, the electro-thermal effect based heating and thermal conduction heating shown a better performance in terms of activation time or consumption efficiency, regarding certain actuator geometries. On the other hand, the low cooling rate is indicated by many researchers as one mean drawback of SMA. As indicated by Mohd Jani et al. (2014), the SMAs have a relatively high heat capacity and density, resulting in lower heat transfer rate and operation bandwidth problem. Base on the literature, the natural air convention seems a common way for SMAs' cooling. One needs to mention that the actuator response time is affected by their size and shape, where ones with lower diameters cool faster due to their higher surface-to-volume ratio. Beyond this method, improvements due to convective condition (force air or liquid convection) and to conductive material (heat skin) were carried out in the literature (see table 2). One need to mention that the modular introduced by Abadie et al. (2002) offered improvement in response time both in heating and cooling. The actuator provided a ten times greater deflection than using the Joule effect and air convection with 1Hz.

5.5 Sensing and controlling methods

As mentioned in the previous section, lack of control accuracy is one of the main disadvantages of SMA actuators. Since the electro-thermal method is usually implemented to activate actuators, the measurement of the actuator's real strain is difficult. Based on the literature, a rotary mechanism embedded with an encoder DC rotary motor is a standard method to measure the actuation system's motion range using SMA wire. For SMA in other forms such as bending sheets or torsional springs, the image processing is often implemented, and it is proven to be a suitable method for motion sensing (see table 2). Beyond this two common methods, one needs to highlight two approaches on sensing of SMA for BTM:
1) SMA wires can be used as self-sensing actuators because its unique hysteresis: the variation of its electric resistance R and the strain of actuator ϵ yield a linear relation due to the changing of its geometry (Ruth et al., 2015; Prechtl et al., 2020);
2) A stretchable mesoscale bending sensor named 'elastic curvature sensor' is presented in (Firouzeh et al., 2013), it is manufactured using carbon impregnated silicone rubber and it is capable of offering a repeatable measurement with a rotation angle up to 150 degrees. Focusing on controlling methods for BTM application, various of methods can be found in the literature. The PI /PID controller have been frequently implemented and have been proven capable for accurately control the SMA-wire-based application ((Moallem and Tabrizi, 2008; Ruth et al., 2015; Guo et al., 2013, 2015; Georges et al., 2013; Doroudchi et al., 2018), for normal-strain-driven application, (Sheng and Desai, 2015; Sheng et al., 2017) for torsional spring, (Shin et al., 2016; Kim et al., 2019) for bending wire).

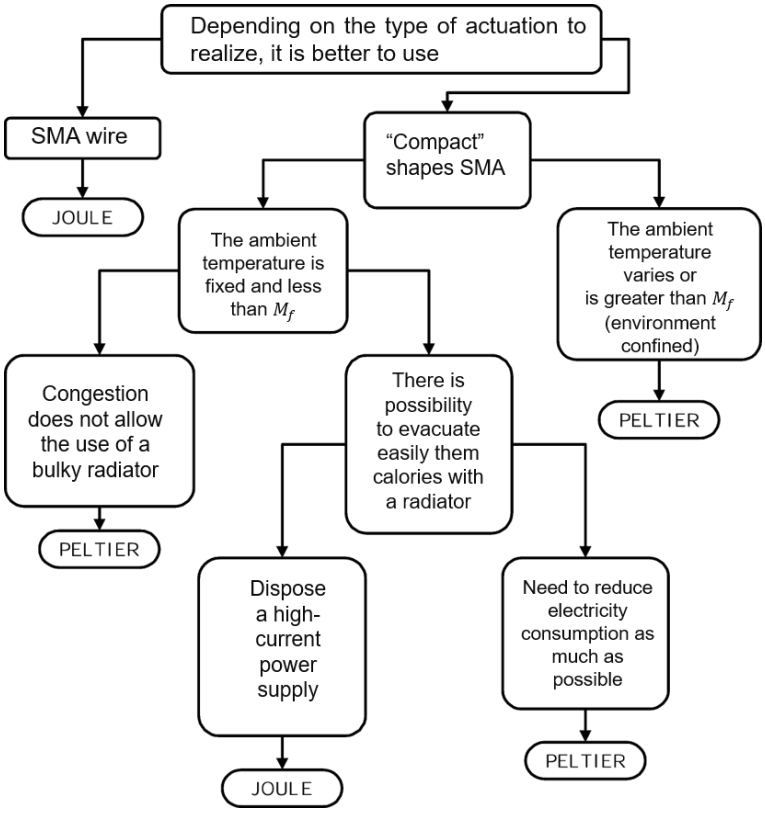

Figure 11. A guideline for determination of activation method of SMA elementary actuator between Joule effect and Peltier effect (Abadie, 2000)

6 CONCLUSION & PERSPECTIVES

This review article summarizes the different types of SMA-based bidirectional torsional motion actuation, where the one-dimensional deformation of the SMA element can be transferred into rotational motion in two opposite directions using various arrangements and temperature control methods. As identified in this review, SMA can play a significant role in realizing BTM in multiple-scales. Classifications are carried out based on various features: elementary SMA for uni-directional torsional motion; passive and active biased actuators for different types of torsional articulation of BTM. The article has presented various summaries of solutions for BTM actuation using thermal-activated SMA elements. The torsional SMA element showed an exciting potential for an application that needs a large rotation angle within limited operational space, such as origami-inspired robotics. Based on the review, discussion regarding various aspects is carried out.

On the other hand, to enhance this exciting approach, several challenges need to be addressed: focusing on analytical tools for actuators prediction, multi-physical reduced-order models have been proven suitable for actuators using simple geometry, but rigorous analysis may need to be more widely applied for reliably capturing of component's mechanical response with complex geometries. Moreover, origami structures exhibit high non linear behaviour. Thus the modelling of such structures and the embedded SMAs have been proven to be a challenge. A summary of SMA elements characterization is introduced, but measurement strategies combining both motion range and output torque of the mesoscale BTM system is still on demand. Based on the discussion of device performance prediction and designing strategies, an inverse model-driven design seems interesting for designing and integrating appropriate actuators on origami structures. Available temperature controlling methods, sensing and controlling tools are discussed.

Significant drawbacks, including large power requirements, relatively low response dynamic due to the cooling method, are illustrated. Perspective can be a complementary study of BTM actuator using active biased torsional SMA element and integrating such actuator for origami structure's shape-changing and shape blocking.

FUNDING

This work was supported by the French National Agency for Research (OrigaBot ANR-18-CE33-0008), and EUR EIPHI (Contract No. ANR-17-EURE-0002)

REFERENCES

Abadie, J. (2000). *Etude et réalisation de micro-actionneurs intégrés à base d'alliage à mémoire de forme*. Theses, Université de Franche-Comté

Abadie, J., Chaillet, N., and Lexcellent, C. (2002). An integrated shape memory alloy micro-actuator controlled by thermoelectric effect. *Sensors and Actuators A: Physical* 99, 297–303. doi:https://doi.org/10.1016/S0924-4247(01)00832-9

Abadie, J., Chaillet, N., and Lexcellent, C. (2009). Modeling of a new sma micro-actuator for active endoscopy applications. *Mechatronics* 19, 437–442. doi:https://doi.org/10.1016/j.mechatronics.2008.11.010

Abeyaratne, R., Sang-Joo, K., and Knowles, J. K. (1994). A one-dimensional continuum model for shape-memory alloys. *International Journal of Solids and Structures* 31, 2229–2249. doi:https://doi.org/10.1016/0020-7683(94)90208-9

An, S.-M., Ryu, J., Cho, M., and Cho, K.-J. (2012). Engineering design framework for a shape memory alloy coil spring actuator using a static two-state model. *Smart Materials and Structures* 21, 055009. doi:10.1088/0964-1726/21/5/055009

Barbarino, S. (2015). Chapter 7 - smas in commercial codes. In *Shape Memory Alloy Engineering*, eds. L. Lecce and A. Concilio (Boston: Butterworth-Heinemann). 193–212. doi:https://doi.org/10.1016/B978-0-08-099920-3.00007-3

Basaeri, H., Yousefi-Koma, A., Zakerzadeh, M. R., and Mohtasebi, S. S. (2014). Experimental study of a bio-inspired robotic morphing wing mechanism actuated by shape memory alloy wires. *Mechatronics* 24, 1231–1241. doi:https://doi.org/10.1016/j.mechatronics.2014.10.010

Benafan, O., Moholt, M., Bass, M., Mabe, J., Nicholson, D., and Calkins, F. (2019). Recent advancements in rotary shape memory alloy actuators for aeronautics. *Shape Memory and Superelasticity* 5, 415–428. doi:https://doi.org/10.1007/s40830-019-00260-3

Benouhiba, A., Rabenorosoa, K., Rougeot, P., Ouisse, M., and Andreff, N. (2018). A multisegment electro-active polymer based milli-continuum soft robots. In *2018 IEEE/RSJ International Conference on Intelligent Robots and Systems (IROS)*. 7500–7506. doi:10.1109/IROS.2018.8593609

Bhandari, B., Lee, G.-Y., and Ahn, S.-H. (2012). A review on ipmc material as actuators and sensors: Fabrications, characteristics and applications. *International Journal of Precision Engineering and Manufacturing* 13, 141–163. doi:10.1007/s12541-012-0020-8

Brinson, L. C. (1993). One-dimensional constitutive behavior of shape memory alloys: thermomechanical derivation with non-constant material functions and redefined martensite internal variable. *Journal of Intelligent Material Systems and Structures* 4, 229–242. doi:https://doi.org/10.1177/1045389X9300400213

Buehler, W. J., Gilfrich, J. V., and Wiley, R. (1963). Effect of low-temperature phase changes on the mechanical properties of alloys near composition tini. *Journal of applied physics* 34, 1475–1477.

doi:10.1063/1.1729603

Bundhoo, V., Haslam, E., Birch, B., and Park, E. J. (2009). A shape memory alloy-based tendon-driven actuation system for biomimetic artificial fingers, part i: design and evaluation. *Robotica* 27, 131–146. doi:10.1017/S026357470800458X

Chapman, C., Eshghinejad, A., and Elahinia, M. (2011). Torsional behavior of niti wires and tubes: Modeling and experimentation. *Journal of Intelligent Material Systems and Structures* 22, 1239–1248. doi:https://doi.org/10.1177/1045389X11411224

Chung, J.-H., Heo, J.-S., and Lee, J.-J. (2006). Modeling and numerical simulation of the pseudoelastic behavior of shape memory alloy circular rods under tension–torsion combined loading. *Smart Materials and Structures* 15, 1651. doi:10.1088/0964-1726/15/6/018

Churchill, C., Shaw, J., and Iadicola, M. (2009). Tips and tricks for characterizing shape memory alloy wire: Part 2—fundamental isothermal responses. *Experimental Techniques* 33, 51–62. doi:https://doi.org/10.1111/j.1747-1567.2008.00460.x

Cisse, C., Zaki, W., and Zineb, T. B. (2016). A review of constitutive models and modeling techniques for shape memory alloys. *International Journal of Plasticity* 76, 244–284. doi:10.1016/j.ijplas.2015.08.006

Collet, M., Ouisse, M., Foltete, E., and Lexcellent, C. (2009). Isothermal and anisothermal implementations of 2d shape memory alloy modeling for transient impact response calculation. *Smart Materials and Structures* 18, 125019. doi:10.1088/0964-1726/18/12/125019

De Sars, V., Haliyo, S., and Szewczyk, J. (2010). A practical approach to the design and control of active endoscopes. *Mechatronics* 20, 251–264. doi:10.1016/j.mechatronics.2009.12.001

Doaré, O., Sbarra, A., Touzé, C., Moussa, M. O., and Moumni, Z. (2012). Experimental analysis of the quasi-static and dynamic torsional behaviour of shape memory alloys. *International Journal of Solids and Structures* 49, 32–42. doi:10.1016/j.ijsolstr.2011.09.009

Doroudchi, A., Zakerzadeh, M. R., and Baghani, M. (2018). Developing a fast response sma-actuated rotary actuator: modeling and experimental validation. *Meccanica* 53, 305–317. doi:https://doi.org/10.1007/s11012-017-0726-x

Duval, A., Haboussi, M., and Zineb, T. B. (2011). Modelling of localization and propagation of phase transformation in superelastic sma by a gradient nonlocal approach. *International Journal of Solids and Structures* 48, 1879–1893. doi:10.1016/j.ijsolstr.2011.02.019

Dynalloy, I. (2011). Technical characteristics of flexinol actuator wires. *CA: Tustin* 690

Elahinia, M. (2016). *Shape Memory Alloy Actuators: Design, Fabrication and Experimental Evaluation* (John Wiley & Sons). doi:10.1002/9781118426913

Firouzeh, A. and Paik, J. (2015). Robogami: A fully integrated low-profile robotic origami. *Journal of Mechanisms and Robotics* 7. doi:10.1115/1.4029491

Firouzeh, A., Sun, Y., Lee, H., and Paik, J. (2013). Sensor and actuator integrated low-profile robotic origami. In *2013 IEEE/RSJ International Conference on Intelligent Robots and Systems*. 4937–4944. doi:10.1109/IROS.2013.6697069

Fremond, M. (1987). Matériaux à mémoire de forme. *Comptes rendus de l'Académie des sciences. Série 2, Mécanique, Physique, Chimie, Sciences de l'univers, Sciences de la Terre* 304, 239–244

Georges, T., Brailovski, V., and Terriault, P. (2012). Characterization and design of antagonistic shape memory alloy actuators. *Smart Materials and Structures* 21, 035010. doi:https://doi.org/10.1088/0964-1726/21/3/035010

Georges, T., Brailovski, V., and Terriault, P. (2013). Experimental bench for shape memory alloys actuators design and testing. *Experimental Techniques* 37, 24–33. doi:10.1111/j.1747-1567.2011.00777.x

Gilardi, G., Haslam, E., Bundhoo, V., and Park, E. J. (2010). A shape memory alloy based tendon-driven actuation system for biomimetic artificial fingers, part ii: modelling and control. *Robotica* 28, 675–687. doi:10.1017/S0263574709990324

Gilpin, K., Torres-Jara, E., and Rus, D. (2014). *Controlling closed-chain robots with compliant SMA actuators: algorithms and experiments*. 149–163. doi:10.1007/978-3-642-28572-1_11

Guo, Z., Pan, Y., Wee, L. B., and Yu, H. (2015). Design and control of a novel compliant differential shape memory alloy actuator. *Sensors and Actuators A: Physical* 225, 71–80. doi:https://doi.org/10.1016/j.sna.2015.01.016

Guo, Z., Yu, H., and Wee, L.-B. (2013). Design of a novel compliant differential shape memory alloy actuator. In *2013 IEEE/RSJ International Conference on Intelligent Robots and Systems*. 4925–4930. doi:https://doi.org/10.1016/j.sna.2015.01.016

Hartl, D. and Lagoudas, D. (2007). Aerospace applications of shape memory alloys. *Proceedings of the Institution of Mechanical Engineers, Part G: Journal of Aerospace Engineering* 221. doi:10.1243/09544100JAERO211

Hawkes, E., An, B., Benbernou, N. M., Tanaka, H., Kim, S., Demaine, E. D., et al. (2010). Programmable matter by folding. *Proceedings of the National Academy of Sciences* 107, 12441–12445. doi:10.1073/pnas.0914069107

Huang, W. (1998). *Shape memory alloys and their application to actuators for deployable structures*. Theses, University of Cambridge

Huang, W. (2002). On the selection of shape memory alloys for actuators. *Materials & Design* 23, 11–19. doi:https://doi.org/10.1016/S0261-3069(01)00039-5

Ianagui, A. and Tannuri, E. A. (2011). Modeling and control of an antagonistic shape memory alloy actuator. In *21st Brazilian Congress of Mechanical Engineering*

Ikuta, K. (1990). Micro/miniature shape memory alloy actuator. In *Proceedings., IEEE International Conference on Robotics and Automation*. vol. 3, 2156–2161. doi:10.1109/ROBOT.1990.126323

Jani, J. M., Leary, M., and Subic, A. (2014). Shape memory alloys in automotive applications. In *Applied Mechanics and Materials* (Trans Tech Publ), vol. 663, 248–253. doi:10.4028/www.scientific.net/AMM.663.248

Jenkins, P. P. and Landis, G. A. (1995). A rotating arm using shape-memory alloy. In *NASA. Johnson Space Center, The 29th Aerospace Mechanisms Symposium*. 167–171

Jianguo, C., Xiaowei, D., Yuting, Z., Jian, F., and Ya, Z. (2016). Folding behavior of a foldable prismatic mast with kresling origami pattern. *Journal of Mechanisms and Robotics* 8. doi:https://doi.org/10.1115/1.4032098

Khan, M. A. H., Manfredi, L., Velsink, F., Huan, Y., and Cuschieri, A. (2016). Analysis of performance and energy efficiency of thin shape memory alloy wire-based actuators. In *Actuator 2016: 15th International Conference on New Actuators & 9th International Exhibition on Smart Actuators and Drive Systems*. 321–324

Kim, J., Lee, D.-Y., Kim, S.-R., and Cho, K.-J. (2015a). A self-deployable origami structure with locking mechanism induced by buckling effect. In *2015 IEEE International Conference on Robotics and Automation (ICRA)*. 3166–3171. doi:10.1109/ICRA.2015.7139635

Kim, S., Lee, D., Koh, J., and Cho, K. (2016). Fast, compact, and lightweight shape-shifting system composed of distributed self-folding origami modules. In *2016 IEEE International Conference on Robotics and Automation (ICRA)*. 4969–4974. doi:10.1109/ICRA.2016.7487704

Kim, S.-W., Lee, J.-G., An, S., Cho, M., and Cho, K.-J. (2015b). A large-stroke shape memory alloy spring actuator using double-coil configuration. *Smart Materials and Structures* 24, 095014. doi:10.1088/

0964-1726/24/9/095014

Kim, Y., Jang, T., Gurung, H., Mansour, N. A., Ryu, B., and Shin, B. (2019). Bidirectional rotating actuators using shape memory alloy wires. *Sensors and Actuators A: Physical* 295, 512–522. doi:https://doi.org/10.1016/j.sna.2019.05.047

Kirsch, S.-M., Welsch, F., Bevilacqua, D., Naso, D., Seelecke, S., Rizzello, G., et al. (2020). Sma antagonistic-micro-wire bundle: First measurement results. In *ASME 2020 Conference on Smart Materials, Adaptive Structures and Intelligent Systems*. doi:https://doi.org/10.1115/SMASIS2020-2261

Koh, J.-S. and Cho, K.-J. (2013). Omega-shaped inchworm-inspired crawling robot with large-index-and-pitch (lip) sma spring actuators. *IEEE/ASME Transactions on Mechatronics* 18, 419–429. doi:10.1109/TMECH.2012.2211033

Koh, J.-s., Kim, S.-r., and Cho, K.-j. (2014). Self-folding origami using torsion shape memory alloy wire actuators. In *International Design Engineering Technical Conferences and Computers and Information in Engineering Conference*. vol. 46377, V05BT08A043. doi:https://doi.org/10.1115/DETC2014-34822

Kshad, M. A. E. and Naguib, H. E. (2021). Modeling and characterization of viscoelastic origami structures using a temperature variation-based model. *Computers & Structures* 246, 106473. doi:https://doi.org/10.1016/j.compstruc.2020.106473

Kuribayashi, K. (1989). Millimeter-sized joint actuator using a shape memory alloy. *Sensors and Actuators* 20, 57–64. doi:https://doi.org/10.1016/0250-6874(89)87102-1

Lagoudas, D. (2008). *Shape Memory Alloys: Modeling and Engineering Applications*. Springer ebook collection / Chemistry and Materials Science 2005-2008 (Springer US). doi:https://doi.org/10.1007/978-0-387-47685-8

Lan, C.-C., Wang, J.-H., and Fan, C.-H. (2009). Optimal design of rotary manipulators using shape memory alloy wire actuated flexures. *Sensors and Actuators A: Physical* 153, 258–266. doi:https://doi.org/10.1016/j.sna.2009.05.019

Lee, D.-Y., Kim, J.-S., Kim, S., Koh, J.-S., and Cho, K.-J. (2013). The deformable wheel robot using magic-ball origami structure. In *Proceedings of the ASME Design Engineering Technical Conference*. vol. 6. doi:10.1115/DETC2013-13016

Lester, B. T., Baxevanis, T., Chemisky, Y., and Lagoudas, D. C. (2015). Review and perspectives: shape memory alloy composite systems. *Acta Mechanica* 226, 3907–3960. doi:https://doi.org/10.1007/s00707-015-1433-0

Li, S., Fang, H., Sadeghi, S., Bhovad, P., and Wang, K.-W. (2019). Architected origami materials: How folding creates sophisticated mechanical properties. *Advanced Materials* 31, 1805282. doi:https://doi.org/10.1002/adma.201805282

Liang, C. and Rogers, C. A. (1990). One-dimensional thermomechanical constitutive relations for shape memory materials. *Journal of Intelligent Material Systems and Structures* 1, 207–234. doi:10.1177/1045389X9000100205

Liu, X., Liu, H., and Tan, J. (2019). Mesoscale shape memory alloy actuator for visual clarity of surgical cameras in minimally invasive robotic surgery. *IEEE Transactions on Medical Robotics and Bionics* 1, 135–144. doi:10.1109/TMRB.2019.2930752

Lobo, P. S., Almeida, J., and Guerreiro, L. (2015). Shape memory alloys behaviour: a review. *Procedia Engineering* 114, 776–783. doi:https://doi.org/10.1016/j.proeng.2015.08.025

Lucy, M. H. and Center., L. R. (1996). *Report on alternative devices to pyrotechnics on spacecraft*. Tech. rep., NASA Langley Research Center

Mirzaeifar, R., DesRoches, R., and Yavari, A. (2010). Exact solutions for pure torsion of shape memory alloy circular bars. *Mechanics of Materials* 42, 797–806. doi:https://doi.org/10.1016/j.mechmat.2010.

06.003

Moallem, M. and Tabrizi, V. (2008). Tracking control of an antagonistic shape memory alloy actuator pair. *IEEE Transactions on Control Systems Technology* 17, 184–190. doi:10.1109/TCST.2008.922506

Moghadam, M. H., Zakerzadeh, M. R., and Ayati, M. (2019). Development of a cascade position control system for an sma-actuated rotary actuator with improved experimental tracking results. *Journal of the Brazilian Society of Mechanical Sciences and Engineering* 41, 407. doi:10.1007/s40430-019-1896-3

Mohd Jani, J., Leary, M., Subic, A., and Gibson, M. A. (2014). A review of shape memory alloy research, applications and opportunities. *Materials & Design (1980-2015)* 56, 1078–1113. doi:https://doi.org/10.1016/j.matdes.2013.11.084

Nespoli, A., Bassani, E., Besseghini, S., and Villa, E. (2010). Rotational mini-actuator activated by two antagonist shape memory alloy wires. *Physics Procedia* 10, 182–188. doi:https://doi.org/10.1016/j.phpro.2010.11.096

Paik, J. K., Byoungkwon, A., Rus, D., and Wood, R. J. (2012). Robotic origamis: Self-morphing modular robot. In *International Conference on Morphological Computation*

Paik, J. K., Hawkes, E., and Wood, R. J. (2010). A novel low-profile shape memory alloy torsional actuator. *Smart Materials and Structures* 19, 125014. doi:https://doi.org/10.1088/0964-1726/19/12/125014

Paik, J. K., Kramer, R. K., and Wood, R. J. (2011). Stretchable circuits and sensors for robotic origami. In *2011 IEEE/RSJ International Conference on Intelligent Robots and Systems*. 414–420. doi:10.1109/IROS.2011.6094746

Paik, J. K. and Wood, R. J. (2012). A bidirectional shape memory alloy folding actuator. *Smart Materials and Structures* 21, 065013. doi:https://doi.org/10.1088/0964-1726/21/6/065013

Paiva, A. and Savi, M. A. (2006). An overview of constitutive models for shape memory alloys. *Mathematical Problems in Engineering* 2006. doi:10.1155/MPE/2006/56876

Peraza Hernandez, E., Hartl, D., Malak, R., and Lagoudas, D. (2014). Origami-inspired active structures: A synthesis and review. *Smart Materials and Structures* 23, 094001. doi:10.1088/0964-1726/23/9/094001

Peraza-Hernandez, E. A., Hartl, D. J., Jr, R. J. M., and Lagoudas, D. C. (2014). Origami-inspired active structures: a synthesis and review. *Smart Materials and Structures* 23, 094001. doi:10.1088/0964-1726/23/9/094001

Peraza-Hernandez, E. A., Hartl, D. J., and Malak Jr, R. J. (2013). Design and numerical analysis of an sma mesh-based self-folding sheet. *Smart Materials and Structures* 22, 094008. doi:10.1088/0964-1726/22/9/094008

Prahlad, H. and Chopra, I. (2007). Modeling and experimental characterization of sma torsional actuators. *Journal of Intelligent Material Systems and Structures* 18, 29–38. doi:10.1177/1045389X06064349

Prechtl, J., Seelecke, S., Motzki, P., and Rizzello, G. (2020). Self-sensing control of antagonistic sma actuators based on resistance-displacement hysteresis compensation. In *ASME 2020 Conference on Smart Materials, Adaptive Structures and Intelligent Systems*. doi:https://doi.org/10.1115/SMASIS2020-2224

Rao, A., Ruimi, A., and Srinivasa, A. R. (2014). Internal loops in superelastic shape memory alloy wires under torsion–experiments and simulations/predictions. *International Journal of Solids and Structures* 51, 4554–4571. doi:https://doi.org/10.1016/j.ijsolstr.2014.09.002

Redmond, J. A., Brei, D., Luntz, J., Browne, A. L., Johnson, N. L., and Strom, K. A. (2010). The design and experimental validation of an ultrafast shape memory alloy resettable (smart) latch. *Journal of Mechanical Design* 132. doi:https://doi.org/10.1115/1.4001393

Reynaerts, D. and Van Brussel, H. (1998). Design aspects of shape memory actuators. *Mechatronics* 8, 635–656. doi:https://doi.org/10.1016/S0957-4158(98)00023-3

Rodrigue, H., Bhandari, B., Han, M.-W., and Ahn, S.-H. (2015a). A shape memory alloy–based soft morphing actuator capable of pure twisting motion. *Journal of Intelligent Material Systems and Structures* 26, 1071–1078. doi:https://doi.org/10.1177/1045389X14536008

Rodrigue, H., Wang, W., Bhandari, B., Han, M.-W., and Ahn, S.-H. (2015b). Sma-based smart soft composite structure capable of multiple modes of actuation. *Composites Part B: Engineering* 82, 152–158. doi:https://doi.org/10.1016/j.compositesb.2015.08.020

Rodrigue, H., Wang, W., Han, M.-W., Kim, T. J., and Ahn, S.-H. (2017). An overview of shape memory alloy-coupled actuators and robots. *Soft Robotics* 4, 3–15. doi:10.1089/soro.2016.0008

Romano, R. and Tannuri, E. A. (2009). Modeling, control and experimental validation of a novel actuator based on shape memory alloys. *Mechatronics* 19, 1169–1177. doi:https://doi.org/10.1016/j.mechatronics.2009.03.007

Roudaut, A., Karnik, A., Löchtefeld, M., and Subramanian, S. (2013). Morphees: Toward high "shape resolution" in self-actuated flexible mobile devices. In *Proceedings of the SIGCHI Conference on Human Factors in Computing Systems* (New York, NY, USA), CHI '13, 593–602. doi:10.1145/2470654.2470738

Rus, D. and Tolley, M. (2018). Design, fabrication and control of origami robots. *Nature Reviews Materials* 3, 101–112. doi:10.1038/s41578-018-0009-8

Ruth, D. J. S., Dhanalakshmi, K., and Nakshatharan, S. S. (2015). Bidirectional angular control of an integrated sensor/actuator shape memory alloy based system. *Measurement* 69, 210–221. doi:https://doi.org/10.1016/j.measurement.2015.02.058

Salerno, M., Tognarelli, S., Quaglia, C., Dario, P., and Menciassi, A. (2013). Anchoring frame for intra-abdominal surgery. *The International Journal of Robotics Research* 32, 360–370. doi:10.1177/0278364912469672

Saputo, S., Sellitto, A., Battaglia, M., Sebastiano, V., and Riccio, A. (2020). Numerical simulation of the mechanical behaviour of shape memory alloys based actuators. *Materials Today: Proceedings* doi:10.1016/j.matpr.2020.01.185

Sayyaadi, H., Zakerzadeh, M., and Salehi, H. (2012). A comparative analysis of some one-dimensional shape memory alloy constitutive models based on experimental tests. *Scientia Iranica* 19, 249–257. doi:https://doi.org/10.1016/j.scient.2012.01.005

Shahin, A. R., Meckl, P. H., Jones, J. D., and Thrasher, M. A. (1994). Enhanced cooling of shape memory alloy wires using semiconductor "heat pump" modules. *Journal of Intelligent Material Systems and Structures* 5, 95–104. doi:https://doi.org/10.1177/1045389X9400500111

Shaw, J., Churchill, C., and Iadicola, M. (2008). Tips and tricks for characterizing shape memory alloy wire: Part 1—differential scanning calorimetry and basic phenomena. *Experimental Techniques* 32, 55–62. doi:https://doi.org/10.1111/j.1747-1567.2008.00410.x

Shaw, J. A. (2002). A thermomechanical model for a 1-d shape memory alloy wire with propagating instabilities. *International Journal of Solids and Structures* 39, 1275–1305. doi:https://doi.org/10.1016/S0020-7683(01)00242-6

Sheng, J. and Desai, J. P. (2015). Design, modeling and characterization of a novel meso-scale sma-actuated torsion actuator. *Smart Materials and Structures* 24, 105005. doi:https://doi.org/10.1088/0964-1726/24/10/105005

Sheng, J., Gandhi, D., Gullapalli, R., Simard, J. M., and Desai, J. P. (2017). Development of a meso-scale sma-based torsion actuator for image-guided procedures. *IEEE Transactions on Robotics* 33, 240–248. doi:10.1109/TRO.2016.2623348

Shim, J.-E., Quan, Y.-J., Wang, W., Rodrigue, H., Song, S.-H., and Ahn, S.-H. (2015). A smart soft actuator using a single shape memory alloy for twisting actuation. *Smart Materials and Structures* 24, 125033.

doi:https://doi.org/10.1088/0964-1726/24/12/125033

Shin, B. H., Jang, T., Ryu, B.-J., and Kim, Y. (2016). A modular torsional actuator using shape memory alloy wires. *Journal of Intelligent Material Systems and Structures* 27, 1658–1665. doi:https://doi.org/10.1177/1045389X15600084

Song, G. (2007). Design and control of a nitinol wire actuated rotary servo. *Smart Materials and Structures* 16, 1796–1801. doi:10.1088/0964-1726/16/5/034

Stroud, H. and Hartl, D. (2020). Shape memory alloy torsional actuators: a review of applications, experimental investigations, modeling, and design. *Smart Materials and Structures* 29, 113001. doi:10.1088/1361-665X/abbb12

Takeda, K., Tobushi, H., Mitsui, K., Nishimura, Y., and Miyamoto, K. (2012). Torsional properties of tini shape memory alloy tape for rotary actuator. *Journal of Materials Engineering and Performance* 21, 2680–2683. doi:10.1007/s11665-012-0277-1

Tanaka, K. (1986). A thermomechanical sketch of shape memory effect: one-dimensional tensile behavior. *RES MECHANICA* 2, 59–72

Tobushi, H., Pieczyska, E., Miyamoto, K., and Mitsui, K. (2013). Torsional deformation characteristics of tini sma tape and application to rotary actuator. *Journal of Alloys and Compounds* 577, S745–S748. doi:https://doi.org/10.1016/j.jallcom.2011.10.108

Tobushi, H., Pieczyska, E. A., Nowacki, W. K., Date, K., and Miyamoto, K. (2010). Two-way rotary shape memory alloy thin strip actuator. *Journal of Theoretical and Applied Mechanics* 48, 1043–1056

Tobushi, H., Sakuragi, T., and Sugimoto, Y. (2008). Deformation and rotary driving characteristics of a shape-memory alloy thin strip element. *Materials Transactions* 49, 151–157. doi:10.2320/matertrans.MRA2007214

Tolley, M. T., Felton, S. M., Miyashita, S., Aukes, D., Rus, D., and Wood, R. J. (2014). Self-folding origami: shape memory composites activated by uniform heating. *Smart Materials and Structures* 23, 094006. doi:https://doi.org/10.1088/0964-1726/23/9/094006

Velázquez, R., Hafez, M., Pissaloux, E., and Szewczyk, J. (2006). A computational-experimental thermomechanical study of shape memory alloy microcoils and its application to the design of actuators. *Journal of Computational and Theoretical Nanoscience* 3, 538–550. doi:10.1166/jctn.2006.3039

Wang, N., Chaoyu, C., Guo, H., Chen, B., and Zhang, X. (2018). Advances in dielectric elastomer actuation technology. *Science China Technological Sciences* 61, 1512–1527. doi:10.1007/s11431-017-9140-0

Wang, W., Rodrigue, H., and Ahn, S.-H. (2016). Deployable soft composite structures. *Scientific reports* 6, 1–10. doi:https://doi.org/10.1038/srep20869

Wang, Z., Hang, G., Wang, Y., Li, J., and Du, W. (2008). Embedded SMA wire actuated biomimetic fin: a module for biomimetic underwater propulsion. *Smart Materials and Structures* 17, 025039. doi:10.1088/0964-1726/17/2/025039

Wei, Z., Sandstroröm, R., and Miyazaki, S. (1998). Shape-memory materials and hybrid composites for smart systems: Part i shape-memory materials. *Journal of Materials Science* 33, 3743–3762

Wood, L. J., Rendon, J., Malak, R. J., and Hartl, D. (2016). An origami-inspired, sma actuated lifting structure. In *International Design Engineering Technical Conferences and Computers and Information in Engineering Conference*. vol. 50169, V05BT07A024. doi:https://doi.org/10.1115/DETC2016-60261

Yoneyama, T. and Miyazaki, S. (2008). *Shape Memory Alloys for Biomedical Applications*

Yuan, H., Balandraud, X., Fauroux, J., and Chapelle, F. (2017a). Compliant rotary actuator driven by shape memory alloy. In *New Advances in Mechanisms, Mechanical Transmissions and Robotics* (Springer). 343–350. doi:10.1007/978-3-319-45450-4_34

Yuan, H., Fauroux, J.-c., Chapelle, F., and Balandraud, X. (2017b). A review of rotary actuators based on shape memory alloys. *Journal of Intelligent Material Systems and Structures* 28, 1863–1885. doi:10.1177/1045389X16682848

Zhakypov, Z., Belke, C. H., and Paik, J. (2017). Tribot: A deployable, self-righting and multi-locomotive origami robot. In *2017 IEEE/RSJ International Conference on Intelligent Robots and Systems (IROS)*. 5580–5586. doi:10.1109/IROS.2017.8206445

Zhakypov, Z., Falahi, M., Shah, M., and Paik, J. (2015). The design and control of the multi-modal locomotion origami robot, tribot. In *2015 IEEE/RSJ International Conference on Intelligent Robots and Systems (IROS)*. 4349–4355. doi:10.1109/IROS.2015.7353994

Zhakypov, Z., Huang, J.-L., and Paik, J. (2016). A novel torsional shape memory alloy actuator: Modeling, characterization, and control. *IEEE Robotics & Automation Magazine* 23, 65–74. doi:10.1109/MRA.2016.2582868

Zhakypov, Z. and Paik, J. (2018). Design methodology for constructing multimaterial origami robots and machines. *IEEE Transactions on Robotics* 34, 151–165. doi:10.1109/TRO.2017.2775655

Zhu, P., Brinson, L. C., Peraza-Hernandez, E., Hartl, D., and Stebner, A. (2013). Comparison of three-dimensional shape memory alloy constitutive models: finite element analysis of actuation and superelastic responses of a shape memory alloy tube. In *Smart Materials, Adaptive Structures and Intelligent Systems*. vol. 2, V002T02A004. doi:10.1115/SMASIS2013-3093

Table 2. Summary of existing SMA-based actuation system for BTM

Elementary SMA type[1]	Dimension[2]		Performance[3]		Heating & cooling[4]		Model[5]	Sensing & Controlling[6]		
	D	L	MR	OT				CM[7]	TS[8]	MS[9]
L-SMA (Liu et al., 2019)	-	80	90	-	JH	NAC	LRM/BM	MOSFET	TM	VA
L-SMA (Khan et al., 2016)	0,076	85	60	-	JH	NAC	-	PID	-	RE
T-SMA (Basaeri et al., 2014)	0,254	-	20	-	JH	NAC	LRM/BM	-	-	RE
T-SMA (Redmond et al., 2010)	0,038	-	20	-	JH	NAC	-	-	-	RE
T-SMA (Song, 2007)	0,38	736	30	-	JH	FAC	-	PID	-	RE
T-SMA (Takeda et al., 2012)	0,25	40	90	4	EH	NAC	EXP-driven	-	-	-
T-SMA (Yuan et al., 2017a)	1	753	200	-	JH	-	-	-	-	IP
L-SMA (Bundhoo et al., 2009)	0,035	385	80	2	JH	NAC	LRM/BM	PWM-PID	TC	RE
L-SMA (Kirsch et al., 2020)	0,025	550	31	-	JH	NAC	-	-	-	RE
L-SMA (Guo et al., 2015)	0,25	370	30	-	JH	NAC	LRM/BM	PI	-	RE
L-SMA (Ruth et al., 2015)	1	700	60	1,4	JH	NAC	EXP-driven	SMC	-	-
L-SMA (Doroudchi et al., 2018)	0,2	500	40	-	JH	NAC	LRM/BM	Open-loop	-	RE
L-SMA (Ianagui and Tannuri, 2011)	0,2	150	14	2	JH	PEC	IM	Close-loop	-	RE
L-SMA (Moghadam et al., 2019)	0,2	500	20	20	JH	NAC	LRM/BM	SMC		RE
L-SMA (Nespoli et al., 2010)	0,2	-	160	0,1	JH	NAC	-	-	-	-
L-SMA (Moallem and Tabrizi, 2008)	0,38	964,5	20	15	JH	NAC	LRM/BM	PID		RE
L-SMA (Lan et al., 2009)	0,125	-	14	-	JH	NAC	-	PID	-	RE
L-SMA (De Sars et al., 2010)	0,22	-	10	17	JH	NAC	FEM	SMC	-	-
L-SMA (Rodrigue et al., 2015a)	0,15	100	120	-	JH	-	LRM/BM	-	-	IP
B-SMA (Firouzeh and Paik, 2015)	0,1	4,5	60	0,83	EH	NAC	EXP-driven	Close-loop	IR camera	BS
B-SMA (Gilpin et al., 2014)	0,51	17	60	0,94	JH	HS	-	Close-loop	-	AM
B-SMA (Abadie et al., 2009)	0,2	-	50	0,37	TEH	PEC	RLM	-	TC	VA
B-SMA (Kuribayashi, 1989)	0,05	-	80	0,04	-	NAC	EXP-driven	-	-	-
B-SMA (Kim et al., 2019)	0,25	320	100	15	JH	NAC	EXP-driven	PID	IR camera	RE
B-SMA (Wang et al., 2016)	0,15	190	90	-	JH	-	-	-	-	IP
L-SMA (Wang et al., 2008)	0,2	76	240	-	JH	NLC	-	-	-	IP
T-SMA (Sheng et al., 2017)	0,5	-	40	10	JH	NAC	LRM/BM	PI	TM	VA
T-SMA (Koh et al., 2014)	0,4	12	180	-	JH	NAC	LRM/BM	-	IR camera	IP
T-SMA (Kim et al., 2016)	0,25	8	90	-	JH	NAC	LRM/BM	-	-	IP

[1] L-SMA, B-SMA, T-SMA: SMA wire or linear spring elements, SMA Bending elements, SMA torsional element
[2] D, L (mm): SMA element's diameter or thickness, element's length
[3] MR, OT: motion range (degree), output torque (mNm) for BTM actuation system
[4] JH, EH, TEH, FAC, NAC, NLC, HS, PEC: Joule heating, external heater, Thompson effect heating, forced air convection, natural air convection, natural liquid convection, heat skin, Peltier effect cooling
[5] LRM/BM, RLM, IM, FEM, EXP-driven: Liang & Roger or Brinson model, Raniecki & Lexcellent model, Ikuta model, finite element model, model driven by experimental data
[6] CM, TS, MS: controlling methods, temperature sensing methods, motion sensing methods
[7] PID, SMC: proportional–integral–derivative controller, sliding mode controller
[8] TC, TM: thermocouple, thermomister
[9] RE, VA, IP, BS, AM: rotary encoder, video acquisition, image processing, micro-bending-sensor, accelerometer